targets (regulatory associated protein of mTOR [Raptor] and Foxo3a) (Supplementary Materials and Methods) small interfering RNA (siRNA) using Lipofectamine RNAiMAX reagent (Invitrogen) according to the manufacturer's instructions. After 48 hours, cells were cultured in normal or low-amino-acid media for a further 24 hours. The knockdown effect was confirmed by Western blotting.

Chromatin Immunoprecipitation Assay

Detailed experimental procedures are described in the Supplementary Materials and Methods section.

HCV Replication Analysis

pH77S3 is an improved version of pH77S, a plasmid containing the full-length sequence of the genotype 1a H77 strain of HCV with 5 cell culture–adaptive mutations that promote its replication in Huh-7 hepatoma cells.[13] pH77S.3/Gaussia luciferase (GLuc)2A is a related construct in which the GLuc sequence, fused to the 2A autocatalytic protease of foot-and-mouth virus RNA, was inserted in-frame between p7 and NS2[14] (Supplementary Materials and Methods). A signal sequence in GLuc directs its secretion into cell culture media, allowing real-time, dynamic measurements of GLuc expression to be performed without the need for cell lysis.

A 10-μg aliquot of synthetic RNA transcribed from pH77S.3/GLuc2A was used for electroporation. Cells were pulsed at 260 V and 950 μF using the Gene Pulser II apparatus (Bio-Rad Laboratories, Hercules, CA) and plated in fresh normal medium for 12 hours to recover. Cell medium was changed to ×1 DMEM without serum for 8 hours, then changed to low-amino-acid medium containing 0–8 mmol/L BCAA for a further 24 hours. Cells and culture medium were collected and used for GLuc assays, real-time detection PCR, and Western blotting. The number of viable cells was determined by a (3-[4,5-dimethylthiazol-2-yl]-5-[3-carboxymethoxyphenyl]-2-[4-sulfophenyl] -2H-tetrazolium, inner salt) assay (Promega).

Continuously JFH-1–infecting Huh-7 cells were obtained by the infection of Huh-7 cells with JFH-1 cell culture-derived HCV at a multiplicity of infection of 0.01. Cells were maintained in normal medium by passaging every 3–4 days for approximately 6 months. About 20%–30% of the cells consistently were positive for HCV core protein (Supplementary Figure 4). Culture medium of JFH-1–infecting Huh-7 cells was changed to the low-amino-acid medium containing 0–8 mmol/L BCAA for 24 hours. Cells then were collected and used for assays.

Statistical Analysis

Results are expressed as mean ± standard deviation. Significance was tested by 1-way analysis of variance with the Bonferroni method, and differences were considered statistically significant at a P value of less than .05.

Results

Fischer's Ratio as a Predictive Factor for Treatment Response

The clinical characteristics of patients who received Peg-IFN and RBV combination therapy are shown in Table 1 and Supplementary Table 1, and explanations of these characteristics have been described previously.[4] All patients were infected with HCV genotype 1b and had a high viral load (>100 IU/mL). We compared patients with SVR + TR against those with NR, as assessed by the overall plausibility of treatment response groups using Fisher's C statistic as previously described.[4] We included data on the IL-28B polymorphism and plasma amino acid composition (aminogram).

Univariate regression analysis showed that no single amino acid was associated significantly with treatment response; however, using Fischer's ratio, the BCAA (Ile+Leu+Val)/aromatic amino acids (Phe+Tyr) ratio was associated significantly with treatment response (P = .005) (Table 1). Of the 121 patients with IL-28B major type, SVR, TR, and NR were observed in 53%, 37%, and 10%, respectively, and among 33 patients with IL-28B minor type, SVR, TR, and NR were observed in 15%, 17%, and 68%, respectively (P < .001) (data not shown). Fischer's ratio of SVR, TR, and NR was 2.35 ± 0.38, 2.30 ± 0.29, and 2.10 ± 0.31, respectively (P < .015) (data not shown).

We selected IL-28B polymorphism, hepatic ISG expression, fibrosis stage, HCV RNA, interferon sensitivity determining region mutation, and Fischer's ratio as factors for multivariate analysis. Multivariate analysis revealed that the minor type of IL-28B polymorphism (TG or GG at rs8099917) (odds ratio, 19.7; P < .001), advanced fibrosis stage of the liver (F3–4) (odds ratio, 6.35; P = .001), high hepatic ISGs (≧3.5) (odds ratio, 5.26; P = .005), low Fischer's ratio (continuous range, 1.5–3.3) (unit odds, 8.91; P = .011), and presence of ISDR mutation (≦1) (odds ratio, 4.12; P = .019) independently contributed to NR (Table 1).

The distribution of the Fischer's ratio according to fibrosis stage is shown in Supplementary Figure 1. The ratio decreased significantly in advanced fibrosis stage (F3–4) compared with early fibrosis stage (F1). No significant association between major or minor type of IL-28B polymorphism and different fibrosis stages of the liver was observed (Supplementary Figure 1*A*). In early fibrosis (F1–2) (Supplementary Figure 1*B*), 90% (80 of 89) of SVR+TR cases had the major type of IL-28B polymorphism, and 94% (16 of 17) of NR cases had the minor type. However, in the advanced fibrosis stage of the liver (F3–4) (Supplementary Figure 1*C*), 85% (23 of 27) of SVR+TR cases had the major type of IL-28B polymorphism and 50% (10 of 20) of NR cases had the minor type. Thus, in advanced fibrosis stages, factors other than the IL-28B polymorphism appear to contribute to NR. Interestingly, the Fischer's ratio was significantly lower in NR patients than SVR+TR pa-

tients in the advanced fibrosis stage of the liver. Therefore, Fischer's ratio could be an important predictor for NR that is independent of IL-28B polymorphism and histologic stage of the liver.

Fischer's Ratio and mTORC1 Signaling in CH-C Livers

Hepatic gene expression in 91 of 168 patients (Supplementary Table 1) was obtained using Affymetrix genechip analysis as described previously.[4] To examine the relationship between the plasma Fischer's ratio and mTORC1 signaling in the liver we evaluated the expression of key regulatory genes related to mTORC1 signaling. We found that expression of branched chain amino-acid transaminase 1 (BCAT1), an important catalytic enzyme of BCAA, was significantly negatively correlated with Fischer's ratio (Figure 1*A*). This indicates that the plasma Fischer's ratio is regulated in the liver as well as in peripheral muscle. Interestingly, the expression of c-myc, a positive regulator of BCAT1 (Figure 1*C*),[15] was correlated negatively with the Fischer's ratio (Figure 1*B*). The expression of PDCD4, a negative transcriptional target of ribosomal p70 S6 protein kinase (S6K), downstream of mTORC1, was correlated significantly with BCAT1 (Figure 1*D* and *E*). Thus, in CH-C livers, BCAT1 is induced with progressive liver disease and mTORC1 signaling is repressed, a process that might involve c-myc. Fischer's ratio of the plasma therefore can be seen to reflect mTORC1 signaling in the liver.

Impaired IFN Signaling in Huh-7 Cells Grown in Low-Amino-Acid Medium

Recent reports have shown the functional relevance of mTOR on IFN signaling and antiviral responses.[9,10] To evaluate IFN-alfa signaling and the mTOR pathway, we used Huh-7 cells grown in different amino acid conditions (×1 DMEM, ×1/5 DMEM, ×1/30 DMEM, and ×1/100 DMEM). The phosphorylated forms of mTOR (p-mTOR) and S6K (pS6K), an important downstream regulator of mTORC1 signaling, were decreased substantially in ×1/30 DMEM and ×1/100 DMEM (Figure 2*A*). Interestingly, the expression of the phosphorylated form of signal transducer and activator of transcription 1 (pSTAT1), an essential transducer of type 1 IFN signaling, also was decreased in these conditions (Figure 2*A*). Similarly, the expression of p-mTOR and pSTAT1 was repressed significantly in CH-C livers with a low Fischer's ratio compared with those with a high Fischer's ratio (Supplementary Figure 2, Supplementary Table 2).

To examine whether decreased pSTAT1 expression might be owing to repressed mTORC1 signaling, we knocked down the expression of Raptor, a specific subunit of mTORC1. We achieved more than 50% knockdown of Raptor by specific siRNA (Figure 2*B*). Under these conditions, the expression of p-mTOR and pSK6 were repressed, which is consistent with previous reports.[16] The expression of pSTAT1 also was repressed after Raptor knockdown (Figure 2*B*).

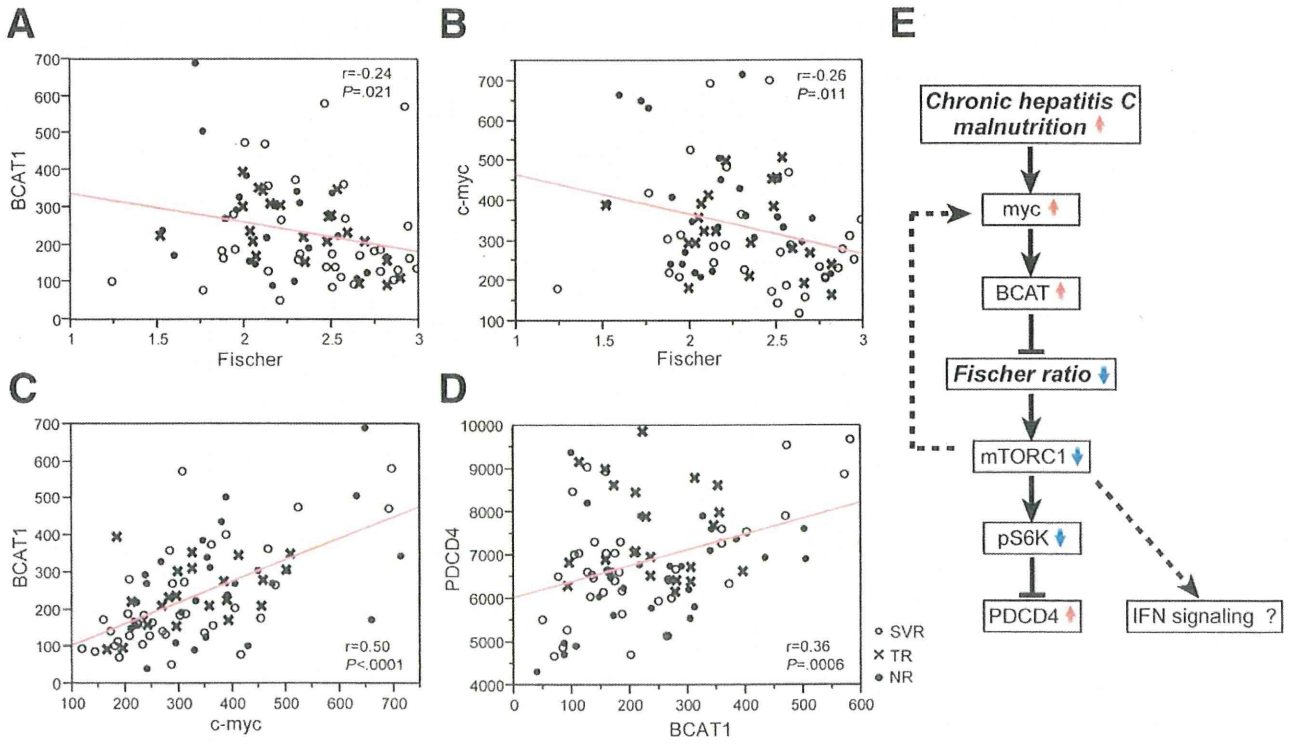

Figure 1. Regression analysis of mTORC1-related gene expression in liver. Gene expression values were determined by probe intensities. (*A*) BCAT1 and Fischer's ratio. (*B*) c-myc and Fischer's ratio. (*C*) BCAT1 and c-myc. (*D*) PDCD4 and BCAT1. (*E*) Putative signaling of mTORC1-related genes in CH-C.

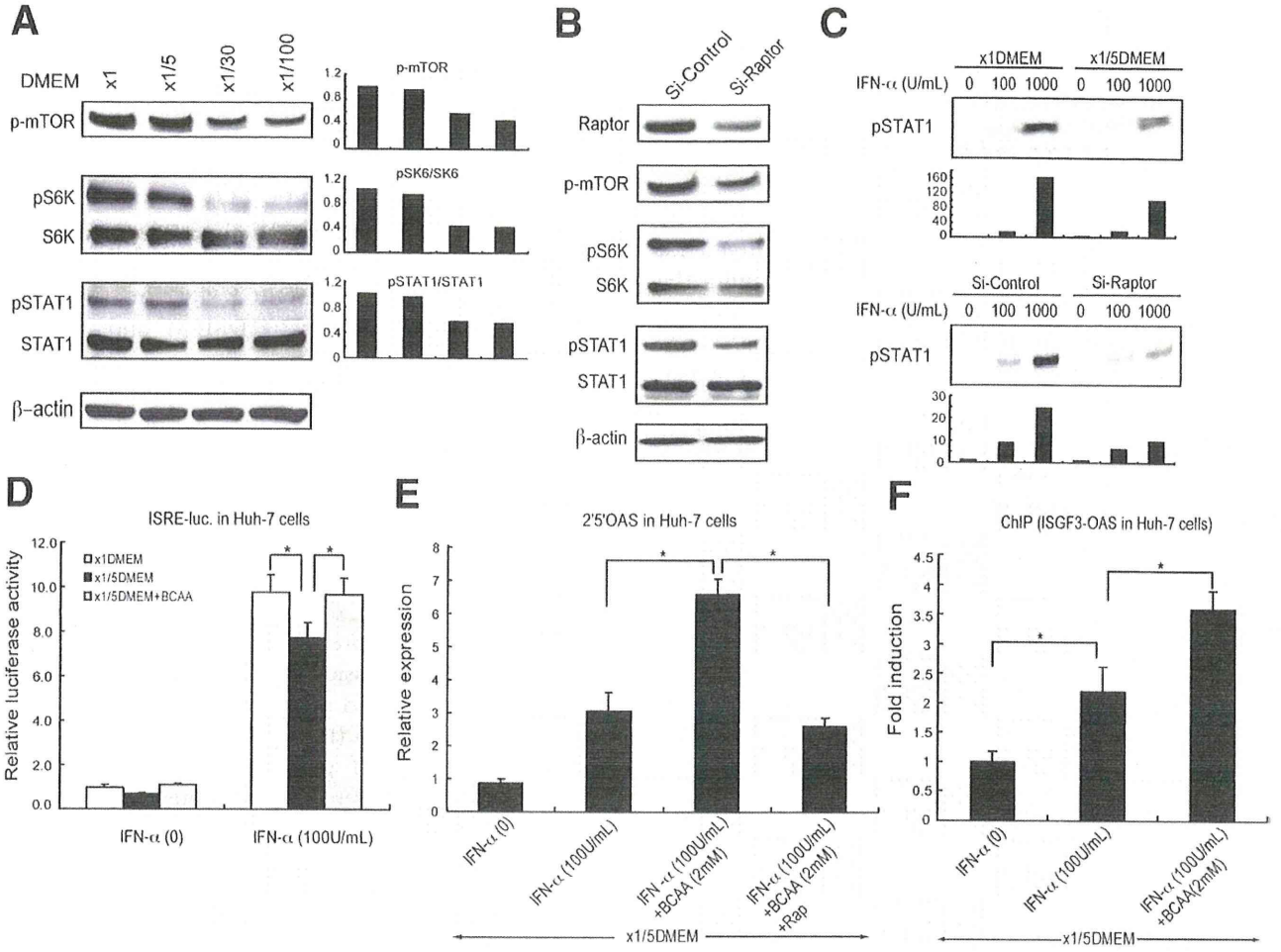

Figure 2. mTORC1 and IFN signaling in Huh-7 cells in low-amino-acid medium. (*A*) p-mTOR, pS6K, and pSTAT1 expression in different amino acid media. (*B*) p-mTOR, pS6K, and pSTAT1 expression under Raptor knock-down conditions. (*C*) IFN-alfa stimulation and pSTAT1 expression in low-amino-acid media or under Raptor knock-down conditions. (*D*) IFN-alfa stimulation and ISRE reporter activities in normal and low-amino-acid media. (*E*) IFN-alfa stimulation and 2'5'OAS expression supplemented with BCAA or rapamycin in low-amino-acid medium. (*F*) Chromatin immunoprecipitation of 2'5'OAS promoter region by ISGF3γ.

The induction of pSTAT1 by IFN-alfa (1000 U/mL) stimulation was impaired in ×1/5 DMEM or in Raptor knocked-down condition, compared with the control (Figure 2*C*). Consistent with these results, IFN-alfa–induced ISRE-dependent transcriptional activity, as measured using an ISRE-luciferase reporter assay, was impaired significantly in ×1/5 DMEM compared with ×1 DMEM (Figure 2*D*). However, this activity could be rescued by the addition of 2 mmol/L BCAA (Figure 2*D*). These results were confirmed by determining the expression of the endogenous IFN-alfa responsive gene, 2'5'OAS, using quantitative reverse-transcription PCR. Figure 2*E* shows that BCAA treatment augmented 2'5'OAS expression in low levels of amino acids, and that this could be reversed by the addition of rapamycin, an inhibitor of mTORC1 (Figure 2*E*). Furthermore, chromatin immunoprecipitation (ChIP) experiments revealed that transcriptional augmentation by BCAA was mediated by the binding of the IFN-alfa–inducible transcription factor, ISGF3γ, to the promoter region of 2'5'OAS (Figure 2*F*). These results indicate that amino acids in culture media play an essential role in IFN-alfa signaling through mTORC1 signaling, and that the addition of BCAA can overcome impaired IFN-alfa signaling in Huh-7 cells.

Induction of Socs3 in Low-Amino-Acid Medium in Huh-7 Cells

Besides being involved in mTOR signaling, Foxo transcriptional factors mediate another important branch of nutrition-sensing signaling pathway.[17] Therefore, we evaluated forkhead box O3A (Foxo3a) expression in low-amino-acid conditions in Huh-7 cells. After 6 hours culture in ×1/5, ×1/30, and ×1/100 DMEM, expression of the phosphorylated form of Foxo3a (pFoxo3a) decreased, whereas that of total Foxo3a increased in ×1/5 and ×1/30 DMEM, and the ratio of pFoxo3a to Foxo3a (pFoxo3a/Foxo3a) substantially decreased (Figure 3*A* and *B*). It has been reported that dephosphorylated Foxo3a is translocated to the nucleus before activation of its target genes.[18] In the present study, immunofluorescent staining

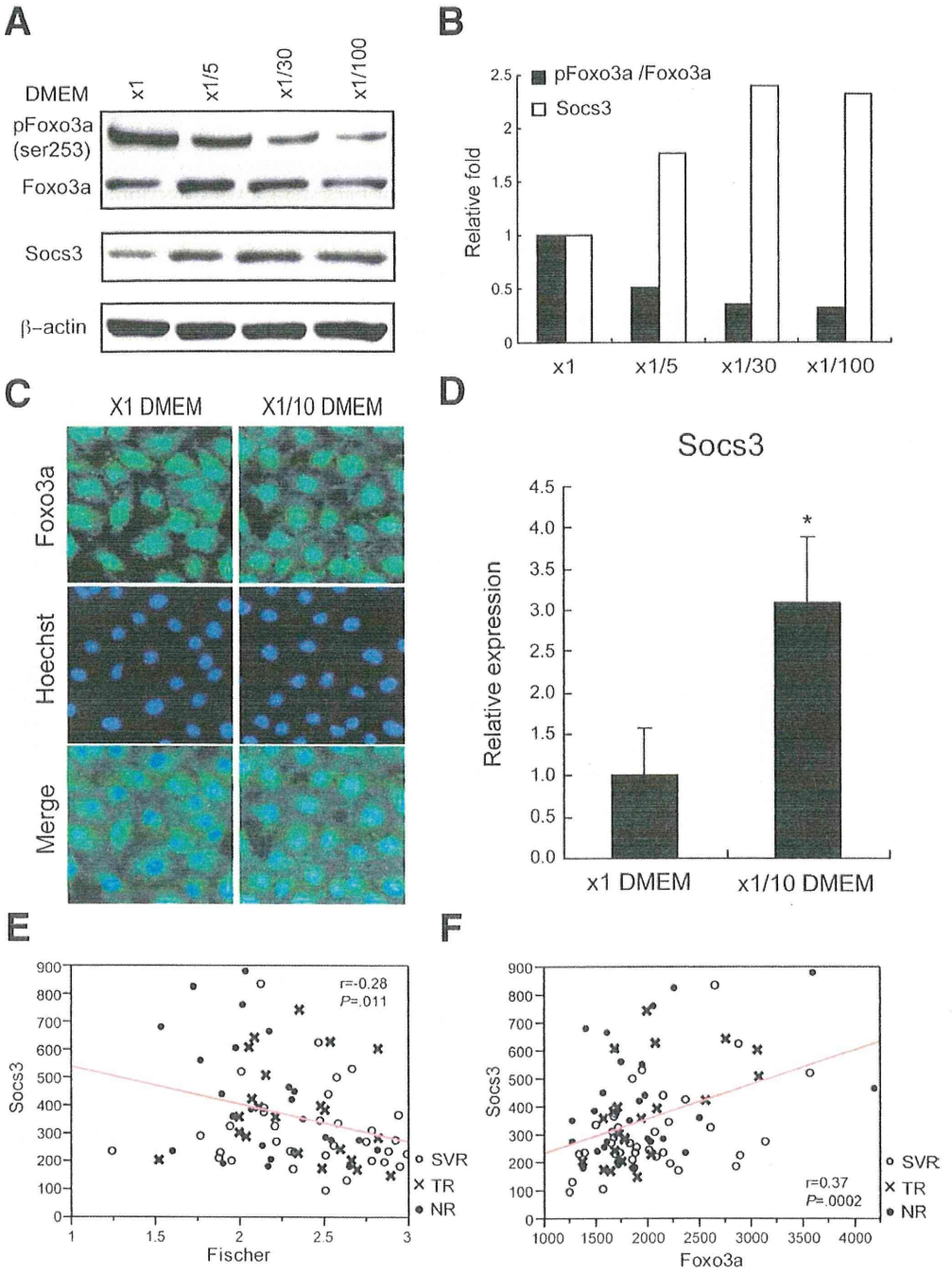

Figure 3. Foxo3a and Socs3 signaling in Huh-7 cells in low-amino-acid medium. (*A*) Foxo3a and Socs3 expression in different amino acid media. (*B*) Relative change of pFoxo3a/Foxo3a and Socs3 expression in different amino acid media. (*C*) Immunofluorescence staining of Foxo3a in Huh-7 cells in normal and low-amino-acid media. (*D*) Relative change of Socs3 messenger RNA in Huh-7 cells in normal and low-amino-acid media. (*E*) Regression analysis of Socs3 in liver and Fischer's ratio. (*F*) Regression analysis of Socs3 and Foxo3a in liver.

with an anti-Foxo3a antibody showed that Foxo3a diffused in both the cytoplasm and nucleus in normal amino acid medium, but localized in the nucleus in low-amino-acid medium (×1/10 DMEM) (Figure 3*C*).

Interestingly, in low-amino-acid medium, transcription and protein expression of Socs3 increased significantly (Figure 3*A*, *B*, and *D*). The induction of Socs3 in a state of malnutrition also was confirmed in clinical samples. In CH-C livers there was a significant negative correlation between the plasma Fischer's ratio and Socs3 expression, implying that Socs3 expression increases during the malnutrition state induced by CH-C. There was also a significant correlation between Foxo3a and the transcriptional level of Socs3 in CH-C livers (Figure 3*E* and *F*), suggesting an in vitro and in vivo biological role for Foxo3a in the activation of Socs3 expression. These findings also were confirmed by Western blotting of CH-C livers (Supplementary Figure 2, Supplementary Table 2).

Socs3 Is a Transcriptional Target of Foxo3a

The significant correlation between Socs3 and Foxo3a in CH-C livers prompted us to analyze the Socs3 promoter sequence and, in doing so, we identified a putative Foxo binding element (FBE) (Figure 4*A*). To investigate the functional relevance of Foxo3a in the transcriptional regulation of Socs3, we constructed reporter plasmids containing a luciferase coding region fused to the Socs3 promoter region (Socs3-luc). Socs3-luc promoter activity was increased substantially by the overexpression of Foxo3a (Figure 4*B*). The mutations introduced in the putative FBE (FBEmut) in the Socs3 promoter significantly reduced Foxo3a-induced Socs3 promoter activation (Figure 4*B*).

Foxo3a then was knocked down by siRNA and Socs3 induction was evaluated. After suppression of Foxo3a (Supplementary Figure 3), Socs3 promoter activity was repressed significantly in low-amino-acid medium (×1/10 DMEM) (Figure 4*C*). Thus, Foxo3a appears to be indispensable for activating the Socs3 promoter under low-amino-acid conditions. Correlating with these results, ChIP assays using an anti-Foxo3a antibody showed a significant increase in the association between Foxo3a and the FBE of the Socs3 promoter in low-amino-acid conditions (×1/10 DMEM) (Figure 4*D*). Taken together, these results suggest that, besides mTORC1 signaling, the Foxo3a-mediated Socs3 signaling pathway might contribute to impaired IFN signaling in a state of malnutrition in CH-C. BCAA potentially restores this signaling (Figure 4*E*).

Effect of BCAA on HCV Replication in Huh-7 or Huh-7.5 Cells

Based on the earlier-described results, we used 2 HCV in vitro replication systems to examine whether BCAA affects HCV replication in Huh-7 or Huh-7.5 cells. The first system used a recombinant infectious genotype 1a clone, H77S.3/GLuc2A (Supplementary Materials and Methods, Supplementary Figure 4), including reporter genes, whereas the second used continuously JFH-1–infecting Huh-7 cells (Supplementary Materials and Methods).

The synthetic RNA transcribed from pH77S.3/GLuc2A was introduced into Huh-7.5 cells and replication of H77S.3/GLuc2A was evaluated in normal or low-amino-acid medium supplemented with BCAA. H77S.3/GLuc2A increased significantly by 2.6-fold in Huh-7.5 cells grown in low-amino-acid medium (×1/5 DMEM) compared with normal amino acid medium (×1 DMEM). Interestingly, BCAA repressed H77S.3/GLuc2A replication in a dose-dependent manner (Figure 5*A*). In agreement with these results, the expression of Mx-1 was increased significantly by the addition of BCAA (Figure 5*B*). Similar findings were observed in JFH-1–infecting Huh-7 cells (Materials and Methods, Supplementary Figure 4). Although no obvious increase in HCV replication was observed in low-amino-acid medium (×1/5 DMEM) compared with normal amino acid medium (×1 DMEM), JFH-1 replication was repressed significantly by the addition of BCAA in a dose-dependent manner (Figure 5*D*). The expression of Mx-1 was increased substantially by the addition of BCAA (Figure 5*E*), suggesting that BCAA significantly repressed HCV replication in cells with either naive or persistent HCV infection. Importantly, there were no significant differences in cell viability between the conditions (Figure 5*C* and *F*).

To validate these findings, signaling pathways in HCV replicating cells were examined (Figure 6*A* and *B*). BCAA increased pS6K in a dose-dependent manner, implying its involvement in the activation of mTORC1 signaling. Related to this, expression of pSTAT1 was shown to be increased and the ratio of pSTAT1 to total STAT1 (pSTAT1/STAT1) increased 2.5- to 3-fold after the addition of BCAA. Thus, BCAA activated mTORC1 and the JAK-STAT signaling pathway in HCV-infected cells. In addition, the expression ratio of pFoxo3a to total Foxo3a (pFoxo3a/Foxo3a) increased 3- to 4-fold, indicating an increase in the cytoplasmic form of Foxo3a that is exposed to proteasome degradation. Concordant with these findings, we observed a decrease in the expression of Socs3. In addition, expression of the HCV core protein decreased as shown in Figure 6*A* and *B*. Thus, these results clearly show that BCAA repressed HCV replication through activation of IFN signaling and repression of Socs3-mediated IFN inhibitory signaling, as proposed in Figure 4*E*.

Discussion

Thompson et al[5] showed that the IL-28B polymorphism, HCV RNA, nationality (Caucasian/Hispanic vs African American), hepatic fibrosis stage, and fasting blood sugar level are all significant variables for achieving SVR in patients infected with genotype 1 HCV. However, the significance of variable factors for treatment response in conjunction with the IL-28B polymorphism has not been evaluated fully. In the present study, in addition to previously examined variables,[4] we included the plasma Fischer's ratio as a nutritional parameter. Multivariate analysis showed that the minor type of IL-28B polymorphism, advanced fibrosis stage, high hepatic ISGs, low Fischer's ratio, and ISDR mutation (≤1) independently contributed to NR (Table 1). Interestingly, among patients of similar fibrosis stage (F3–4), the Fischer's ratio was significantly lower in NR than SVR+TR cases. Therefore, the plasma value of Fischer's ratio was associated with the treatment response that was independent of the IL-28B polymorphism and histologic stage of the liver, although patients with advanced hepatic fibrosis are likely to be nutritionally affected.

As a nutrient sensor signaling pathway, the protein kinase mTOR plays an essential role in maintaining homeostasis and regulates protein synthesis in response to nutrient conditions. mTOR is the catalytic subunit of 2 distinct complexes, mTORC1 and mTORC2. In addition

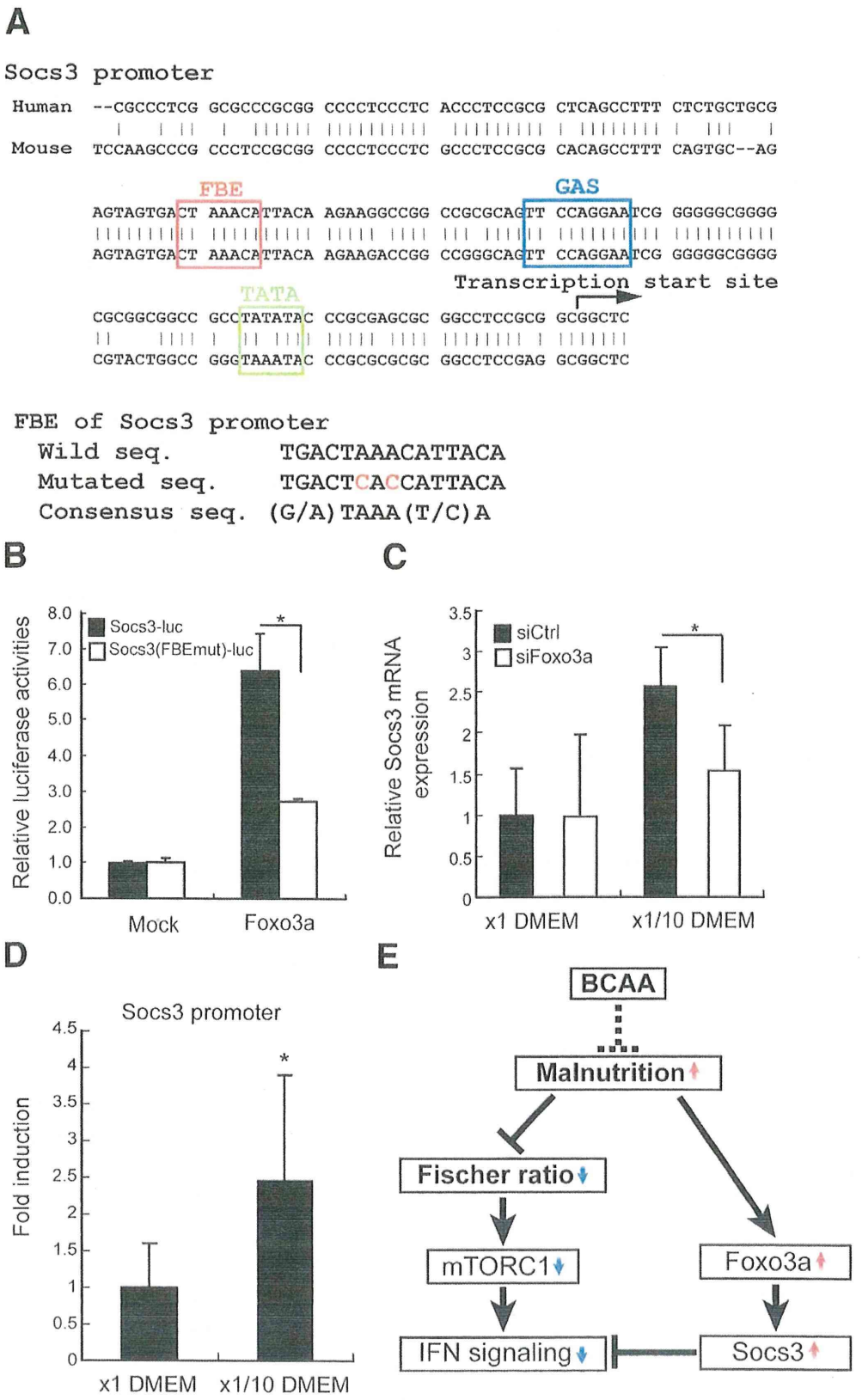

Figure 4. Socs3 promoter assay. (*A*) Primary structure of putative Foxo binding element in Socs3 promoter region. (*B*) Socs3-luc and Socs3 (FBEmut)-luc activities after overexpression of Foxo3a in Huh-7 cells. (*C*) Relative Socs3 messenger RNA (mRNA) expression after knockdown of Foxo3a in normal and low-amino-acid media. (*D*) Chromatin immunoprecipitation of Socs3 promoter region by Foxo3a in normal and low-amino-acid media. (*E*) Model of impaired IFN signaling by repressed mTORC1 signaling and increased Socs3 signaling under CH-C state of malnutrition.

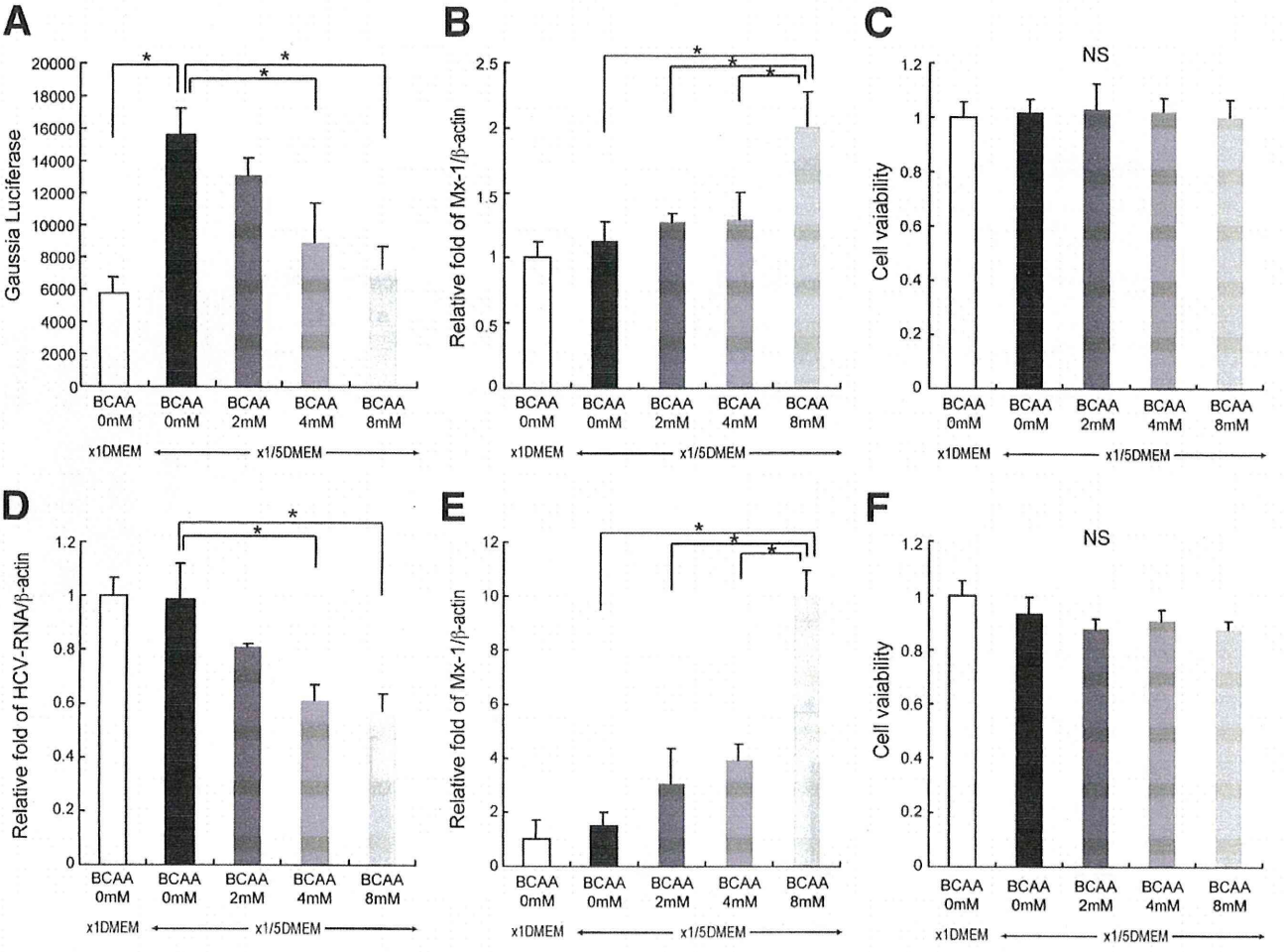

Figure 5. Effect of BCAA on HCV replication in cells in low-amino-acid medium. (*A*) Effect of BCAA on H77S.3/GLuc2A replication in Huh-7.5 cells. (*B*) Mx-1 expression in H77S.3/GLuc2A-transfected Huh-7.5 cells supplemented with BCAA. (*C*) Viability of Huh-7.5 cells. (*D*) Effect of BCAA on JFH-1 replication continuously infecting Huh-7 cells. (*E*) Mx-1 expression in continuously JFH-1–infecting Huh-7 cells supplemented with BCAA. (*F*) Viability of Huh-7 cells.

to these metabolic aspects, recent reports have shown that mTORC1 participates in IFN signaling and antiviral defense responses,[9,10] although the precise signaling pathway has not yet been clarified. In the present study, we evaluated mTORC1 signaling in CH-C livers using gene expression profiling of 91 patients (Figure 1, Supplementary Table 1). We observed a significant negative correlation between plasma Fischer's ratio and hepatic expression of BCAT1, an important catalytic enzyme of BCAA (Figure 1*A*). Moreover, BCAT1 expression was correlated positively with PDCD4 expression, which in turn is regulated negatively by pS6K at the transcriptional level (Figure 1*D*).[16] Thus, the expression of BCAT1 appears to be a negative indicator of mTORC1 signaling in the liver, and the plasma Fischer's ratio is partially reflected by mTORC1 signaling in the liver and muscle.

Interestingly, the expression of c-myc was correlated significantly with BCAT1 (Figure 1C) as reported previously.[15] Several studies observed up-regulated c-myc expression in advanced stages of CH-C[19] but, on the other hand, c-myc recently was shown to be a target of mTORC1 in hepatic cells.[17] The existence of a feedback mechanism between c-myc and mTORC1 signaling to maintain liver homeostasis (Figure 1*E*) is plausible, although the precise mechanisms need to be confirmed.

Impaired mTORC1 signaling is suggested to affect the IFN-alfa–induced signaling pathway. To address this, the relationship between mTORC1 and IFN signaling was assessed using a cell culture system. In low-amino-acid medium (×1/5, ×1/30, and ×1/100 DMEM), expression of pSTAT1 was decreased substantially, correlating with the impaired mTORC1 signaling represented by decreased p-mTOR and pS6K expression in Huh-7 cells (Figure 2*A*).

The relationship between mTORC1 and IFN signaling was confirmed further by the knock-down experiment of Raptor, a specific subunit of mTORC1 (Figure 2*B*), although a more precise analysis should be performed to confirm this relationship. Importantly, when Huh-7 cells were stimulated by IFN-alfa, pSTAT1 induction was repressed significantly in low-amino-acid medium (×1/5 DMEM) or in Raptor knocked-down conditions (Figure 2*C*). It therefore could be speculated that IFN treat-

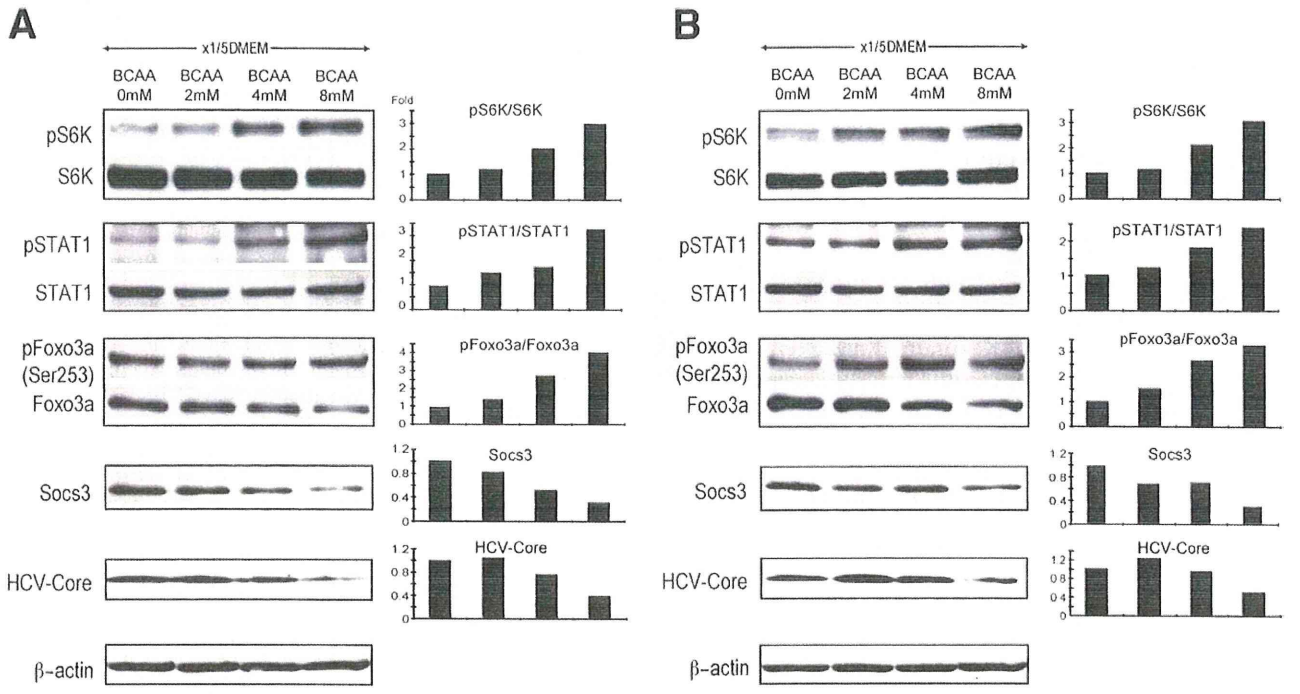

Figure 6. Expression of S6K, STAT1, Foxo3a, Socs3, and HCV core in H77S.3/GLuc2A-transfected Huh-7.5 cells or continuously JFH-1–infecting Huh-7 cells supplemented with BCAA.

ment of patients with liver malnutrition and impaired mTORC1 signaling would lead to reduced induction of ISGs. Importantly, BCAA was able to restore impaired IFN signaling through increased binding of ISGF3γ to its targets (Figure 2*D–F*).

Besides cross-talk of mTORC1 and IFN signaling, we revealed that Foxo3a also is involved in the IFN inhibitory pathway. In low-amino-acid medium, expression of pFoxo3a (ser253) was decreased substantially whereas that of Socs3 was increased. A decreased pFoxo3a/Foxo3a ratio indicates nuclear accumulation of Foxo3a before activation of its target genes, and this was confirmed by immunofluorescent staining (Figure 3C). The expression of Foxo3a was significantly positively correlated with that of Socs3 in CH-C liver (Figure 3*F*). These findings prompted us to identify a putative FBE in the Socs3 promoter region (Figure 4*A*). In fact, Socs3 promoter reporter activity was activated by overexpression of Foxo3a, and mutation of FBE impaired Foxo3a-dependent Socs3 promoter activation. Conversely, induction of Socs3 was not observed when expression of Foxo3a was knocked down by siRNA in low-amino-acid medium. Socs3 induction in low-amino-acid medium was owing to increased binding of Foxo3a to the FBE, which was confirmed by ChIP (Figure 4*D*). Therefore, in addition to impaired mTORC1 signaling, the Foxo3a-mediated Socs3 IFN inhibitory pathway might be involved in impaired IFN signaling in patients with liver malnutrition (Figure 4*E*).

Finally, we examined whether BCAA could restore impaired IFN signaling and inhibit HCV replication in cells under conditions of malnutrition. Importantly, BCAA could repress replication of the recombinant genotype 1a-derived HCV, H77S.3/GLuc2A, in a dose-dependent manner (Figure 5*A*). H77S.3/GLuc2A RNA produces infectious virus[14] and, therefore, the results indicate that BCAA might act on a naive HCV infection. Moreover, BCAA inhibited JFH-1-infected Huh-7 cells in which JFH-1 continuously was infecting in a dose-dependent manner. These results indicate that BCAA had an inhibitory effect on either naive or persistent HCV infection irrespective of genotypes (1a and 2a). Consistent with these results, BCAA induced the expression of pSTAT1 and Mx protein in a dose-dependent manner, and repressed Socs3 expression through increasing the ratio of pFoxo3a (ser243) to Foxo3a in a dose-dependent manner (Figures 5 and 6). Therefore, BCAA potentially could restore impaired IFN signaling and inhibit HCV replication in a CH-C state of malnutrition.

In conclusion, we addressed the clinical significance of the nutritional state of the liver on the treatment response of Peg-IFN and RBV combination therapy for CH-C. Although further studies are required to fully define the precise mechanisms underlying mTOR and IFN signaling, we showed that plasma values of Fischer's ratio are a useful nutritional parameter associated with treatment response. Fischer's ratio reflects mTORC1 signaling in the liver, which is correlated with IFN signaling and related to Socs3 IFN inhibitory signaling through Foxo3a. The potential usefulness of BCAA for the augmentation of IFN signaling could suggest a new therapeutic application for advanced-stage CH-C.

Supplementary Material

Note: To access the supplementary material accompanying this article, visit the online version of *Gastroenterology* at www.gastrojournal.org, and at doi: 10.1053/j.gastro.2011.03.051.

Appendix A

The Hokuriku Liver Study Group is composed of the following members: Drs Takashi Kagaya, Kuniaki Arai, Kaheita Kakinoki, Kazunori Kawaguchi, Hajime Takatori, and Hajime Sunakosaka (Department of Gastroenterology, Kanazawa University Graduate School of Medicine, Kanazawa, Japan); Drs Touru Nakahama and Shinji Kamiyamamoto (Kurobe City Hospital, Kurobe, Toyama, Japan); Dr Yasuhiro Takemori (Toyama Rosai Hospital, Uozu, Toyama, Japan); Dr Hikaru Oguri (Koseiren Namerikawa Hospital, Namerikawa, Toyama, Japan); Drs Yatsugi Noda and Hidero Ogino (Toyama Prefectural Central Hospital, Toyama, Japan); Drs Yoshinobu Hinoue and Keiji Minouchi (Toyama City Hospital, Toyama, Japan); Dr Nobuyuki Hirai (Koseiren Takaoka Hospital, Takaoka, Toyama, Japan); Drs Tatsuho Sugimoto and Koji Adachi (Tonami General Hospital, Tonam, Toyama, Japan); Dr Yuichi Nakamura (Noto General Hospital, Nanao, Ishikawa, Japan); Drs Masashi Unoura and Ryuhei Nishino (Public Hakui Hospital, Hakui, Ishikawa, Japan); Drs Hideo Morimoto and Hajime Ohta (National Hospital Organization Kanazawa Medical Center, Kanazawa, Ishikawa, Japan); Dr Hirokazu Tsuji (Kanazawa Municipal Hospital, Kanazawa, Ishikawa, Japan); Drs Akira Iwata and Shuichi Terasaki (Kanazawa Red Cross Hospital, Kanazawa, Ishikawa, Japan); Drs Tokio Wakabayashi and Yukihiro Shirota (Saiseikai Kanazawa Hospital, Kanazawa, Ishikawa, Japan); Drs Takeshi Urabe and Hiroshi Kawai (Public Central Hospital of Matto Ishikawa, Hakusan, Ishikawa, Japan); Dr Yasutsugu Mizuno (Nomi Municipal Hospital, Nomi, Ishikawa, Japan); Dr Shoni Kameda (Komatsu Municipal Hospital, Komatsu Ishikawa, Japan); Drs Hirotoshi Miyamori and Uichiro Fuchizaki (Keiju Medical Center, Nanao, Ishikawa, Japan); Dr Haruhiko Shyugo (Kanazawa Arimatsu Hospital, Kanazawa, Ishikawa, Japan); Dr Hideki Osaka (Yawata Medical Center, Komatsu, Ishikawa, Japan); Dr Eiki Matsushita (Kahoku Central Hospital, Tsubata, Ishikawa, Japan); Dr Yasuhiro Katou (Katou Hospital, Komatsu, Ishikawa, Japan); Drs Nobuyoshi Tanaka and Kazuo Notsumata (Fukuiken Saiseikai Hospital, Fukui, Japan); Dr Mikio Kumagai (Kumagai Clinic, Tsuruga, Fukui, Japan); and Dr Manabu Yoneshima (Municipal Tsuruga Hospital, Tsuruga, Fukui, Japan).

References

1. Fried MW, Shiffman ML, Reddy KR, et al. Peginterferon alfa-2a plus ribavirin for chronic hepatitis C virus infection. N Engl J Med 2002;347:975–982.
2. Tanaka Y, Nishida N, Sugiyama M, et al. Genome-wide association of IL28B with response to pegylated interferon-alpha and ribavirin therapy for chronic hepatitis C. Nat Genet 2009;41:1105–1109.
3. Ge D, Fellay J, Thompson AJ, et al. Genetic variation in IL28B predicts hepatitis C treatment-induced viral clearance. Nature 2009;461:399–401.
4. Honda M, Sakai A, Yamashita T, et al. Hepatic ISG expression is associated with genetic variation in interleukin 28B and the outcome of IFN therapy for chronic hepatitis C. Gastroenterology 2010;139:499–509.
5. Thompson AJ, Muir AJ, Sulkowski MS, et al. Interleukin-28B polymorphism improves viral kinetics and is the strongest pretreatment predictor of sustained virologic response in genotype 1 hepatitis C virus. Gastroenterology 2010;139:120–129 e18.
6. Nishitani S, Ijichi C, Takehana K, et al. Pharmacological activities of branched-chain amino acids: specificity of tissue and signal transduction. Biochem Biophys Res Commun 2004;313:387–389.
7. Matsumura T, Morinaga Y, Fujitani S, et al. Oral administration of branched-chain amino acids activates the mTOR signal in cirrhotic rat liver. Hepatol Res 2005;33:27–32.
8. Kim DH, Sarbassov DD, Ali SM, et al. mTOR interacts with raptor to form a nutrient-sensitive complex that signals to the cell growth machinery. Cell 2002;110:163–175.
9. Colina R, Costa-Mattioli M, Dowling RJ, et al. Translational control of the innate immune response through IRF-7. Nature 2008;452:323–328.
10. Kaur S, Lal L, Sassano A, et al. Regulatory effects of mammalian target of rapamycin-activated pathways in type I and II interferon signaling. J Biol Chem 2007;282:1757–1768.
11. Shimbo K, Kubo S, Harada Y, et al. Automated precolumn derivatization system for analyzing physiological amino acids by liquid chromatography/mass spectrometry. Biomed Chromatogr 2009;24:683–691.
12. Shirasaki T, Honda M, Mizuno H, et al. La protein required for internal ribosome entry site-directed translation is a potential therapeutic target for hepatitis C virus replication. J Infect Dis 2010;202:75–85.
13. Yi M, Villanueva RA, Thomas DL, et al. Production of infectious genotype 1a hepatitis C virus (Hutchinson strain) in cultured human hepatoma cells. Proc Natl Acad Sci U S A 2006;103:2310–2315.
14. Shimakami T, Welsch C, Yamane D, et al. Protease inhibitor-resistant hepatitis C virus mutants with reduced fitness from impaired production of infectious virus. Gastroenterology 2011;140:667–675.
15. Eden A, Simchen G, Benvenisty N. Two yeast homologs of ECA39, a target for c-Myc regulation, code for cytosolic and mitochondrial branched-chain amino acid aminotransferases. J Biol Chem 1996;271:20242–2045.
16. Dowling RJ, Topisirovic I, Alain T, et al. mTORC1-mediated cell proliferation, but not cell growth, controlled by the 4E-BPs. Science 2010;328:1172–1176.
17. Teleman AA, Hietakangas V, Sayadian AC, et al. Nutritional control of protein biosynthetic capacity by insulin via Myc in Drosophila. Cell Metab 2008;7:21–32.
18. Zhang X, Gan L, Pan H, et al. Phosphorylation of serine 256 suppresses transactivation by FKHR (FOXO1) by multiple mechanisms. Direct and indirect effects on nuclear/cytoplasmic shuttling and DNA binding. J Biol Chem 2002;277:45276–45284.
19. Farinati F, Cardin R, Bortolami M, et al. Oxidative damage, pro-inflammatory cytokines, TGF-alpha and c-myc in chronic HCV-related hepatitis and cirrhosis. World J Gastroenterol 2006;12:2065–2069.

Received October 19, 2010. Accepted March 18, 2011.

Reprint requests

Address requests for reprints to: Shuchi Kaneko, MD, PhD, Department of Gastroenterology, Graduate School of Medicine, Kanazawa University, Takara-Machi 13-1, Kanazawa 920-8641, Japan. e-mail: skaneko@m-kanazawa.jp; e-mail: fax: (81) 76-234-4250.

Acknowledgments

Participating investigators from the Hokuriku Liver Study Group are listed in Appendix A.

The authors thank Mina Nishiyama and Yuki Hatayama for excellent technical assistance.

Conflicts of interest

The authors disclose no conflicts.

Supplementary Materials and Methods

Plasma Amino Acid Analysis

Plasma sample amino acid concentrations were measured by high-performance liquid chromatography–electrospray ionization–mass spectrometry followed by derivatization.[1] An MSQ Plus LC/MS system (Thermo Fischer Scientific, Waltham, MA) equipped with an electrospray ionization source was used in positive ionization mode for selected ion monitoring. Xcalibur version 1.4 SR1 software (Thermo Fischer Scientific, Yokohama, Japan) was used for data collection and processing. The high-performance liquid chromatography separation system consisted of an L-2100 pump, L-2200 autosampler, and L-2300 column oven (Hitachi High-Technologies Corporation, Tokyo, Japan). A Wakosil-II 3C8-100HG column (100, 2.1, 3 mm; Wako Pure Chemical Industries, Osaka, Japan) was used for the separation, and the mobile phase consisted of eluent A (25-mmol/L ammonium formate in water, pH 6.0) and eluent B (water:acetonitrile = 40:60).

Western Blotting

The expression of HCV core protein, Socs3, Foxo3a, phospho-Foxo3a (Ser253) (pFoxo3a), STAT1, pSTAT1 (Tyr701), S6K, pS6K, p-mTOR (Ser2448), Raptor, and β-actin were evaluated with mouse anti-core (Affinity BioReagents, Golden, CO), mouse anti-Socs3 (Santa Cruz Biotechnology, Santa Cruz, CA), rabbit anti-Foxo3a, rabbit anti-β-actin (Sigma-Aldrich, St Louis, MO), rabbit anti-phospho-Foxo3a (Ser253), rabbit anti-STAT1, rabbit anti-p-STAT1 (Tyr701), rabbit anti-p70 S6K, rabbit anti-pS6K, rabbit anti-p-mTOR (Ser2448), and rabbit anti-Raptor (Cell Signaling Technology, Beverly, MA), respectively. Densitometric analysis was conducted directly on the blotted membrane using a charge coupled device camera system (LAS-3000 Mini; Fujifilm, Tokyo, Japan) and Scion Image software (Frederick, MD).

Primer Sequences for PCR and siRNA

Primer sequences for PCR and siRNA were as follows: 2′5′OAS: forward 5′- CTC AGA AAT ACC CCA GCC AAA TC-3′, reverse 5′-GTG GTG AGA GGA CTG AGG AA-3′; Socs3: forward 5′-TAC CAC CTG AGT CTC CAG CTT CTC-3′, reverse 5′-CCT GGC AGT TCT CAT TAG TTC AGC ATT C-3′; Foxo3a: forward 5′-TGC TGT ATG CAA GAA CTT TCC AGT AGC AG-3′, reverse 5′-ACT CTA GCC CCC ATG CTA CTA GTG-3′; glyceraldehyde-3-phosphate dehydrogenase: forward 5′-GAA GGT GAA GGT CGG AGT-3′, reverse 5′-GAA GAT GGT GAT GGG ATT TC-3′, siFoxo3a (SASI_Hs01_00119127; Sigma) sense: 5′-GAA UGA UGG GCU GAC UGA AdTdT-3′, antisense: 5′-UUC AGU CAG CCC AUC AUU CdTdT-3′. Small interfering Raptor was purchased as part of KIAA1303 siGENOME SMART pool siRNA reagents from Dharmacon, Inc (Lafayette, CO).

Construction of ISRE-Luc Reporter and FBEmut-luc Reporter Plasmids

Oligonucleotides containing the ISRE tandem repeat sequence (sense 5′-TCG AGA ACT GAA ACT GAA ACT GAA ACT GAA ACT GAA ACT GAA ACT GAA ACT GAA A-3′, antisense 5′-AGC TTT TCA GTT TCA GTT TCA GTT TCA GTT TCA GTT TCA GTT TCA GTT TCA GTT C-3′, consensus 5′-GAA Ann GAA ACT-3′) were annealed, and integrated into Xho I and Hind III sites of the pGL4.23 luciferase vector (Promega). The human Socs3 promoter region (-109/+217) was amplified by genomic PCR using specific primers (forward, 5′-TGC TGC GAG TAG TGA CTA AAC ATT ACA AG-3′ and reverse, 5′-CCG TGA AGT CCA CAA AGG AGC CTT C-3′) and cloned into the EcoR V site of the pGL4.10-luc2 reporter vector (Promega). The Socs3 FBE mutant reporter vector was created by substituting 2 adenines in the putative FBE with guanines (wild-type sequence 5′-CTAAACA-3′, mutated sequence 5′-CTGAGCA-3′).

ChIP Assay

For the ChIP assay using the anti-ISGF3γ antibody, 1×10^6 Huh-7 cells were treated with IFN-alfa (0 or 100 U/mL) and BCAA (2 mmol/L) in low-amino-acid medium for 6 hours. For ChIP using the anti-Foxo3a antibody, 1×10^6 Huh-7 cells were cultured in low-amino-acid medium for 24 hours.

Cells were cross-linked with 1% formaldehyde in PBS for 10 minutes at 37°C, and the reaction was stopped with 250 mmol/L glycine for 10 minutes. Cells were suspended in sodium dodecyl sulfate–lysis buffer (1% sodium dodecyl sulfate, 10 mmol/L ethylenediaminetetraacetic acid [EDTA], 50 mmol/L Tris-HCl [pH 8.1]), complete protease inhibitor cocktail (Roche Applied Science), and incubated for 30 minutes at 10°C. Cell lysate was sonicated with Bioruptor (Cosmo Bio, Tokyo, Japan) to obtain chromatin fragments and diluted 10-fold in ChIP dilution buffer (0.01% sodium dodecyl sulfate, 1.1% Triton-X 100, 1.2 mmol/L EDTA, 16.7 mmol/L Tris-HCl [pH 8.1], 150 mmol/L NaCl, complete protease inhibitor cocktail). Chromatin fragments were incubated with 2 μg ISGF3γ antibody (Santa Cruz Biotechnology), 2 μg Foxo3a antibody (H-144; Santa Cruz Biotechnology), or normal rabbit immunoglobulin G for 18 hours at 4°C. Dynabeads (30 μL) protein G (Invitrogen) was added and incubated for 1 hour at 4°C. The beads were washed with low-salt-wash buffer (0.1% sodium dodecyl sulfate, 1% Triton-X 100, 2.0 mmol/L EDTA, 20 mmol/L Tris-HCl [pH 8.1], 150 mmol/L NaCl), high-salt-wash buffer (0.1% sodium dodecyl sulfate, 1% Triton-X 100, 2.0 mmol/L EDTA, 20 mmol/L Tris-HCl [pH 8.1], 500 mmol/L NaCl), LiCl wash buffer (250 mmol/L LiCl, 1% NP-40, 1% de-

oxycholate, 1.0 mmol/L EDTA, 1.0 mmol/L Tris-HCl [pH 8.1]) and Tris-EDTA buffer. Immunoprecipitated chromatin fragments were eluted with elution buffer (1% sodium dodecyl sulfate, 100 mmol/L NaHCO3, 10 mmol/L dithiothreitol), and reverse cross-linked by incubating for 6 hours at 65°C in elution buffer containing 200 mmol/L NaCl. DNA fragments were purified and quantified by real-time detection PCR with primers for putative ISRE in the 2′5′OAS promoter region (forward, 5′-AAA TGC ATT TCC AGA GCA GAG TTC AGA G-3′, reverse, 5′-GGG TAT TTC TGA GAT CCA TCA TTG ACA GG-3′) or putative FBE in the Socs3 promoter region (forward, 5′-TGC TGC GAG TAG TGA CTA AAC ATT ACA AG -3′, reverse, 5′-AGC GGA GCA GGG AGT CCA AGT C -3′). Values were normalized by the measurement of input DNA.

pH77S.3/GLuc2A

pH77S.2 is a modification of pH77S[2] containing an additional mutation within the E2 protein (N476D in the polyprotein) that promotes infectious virus yields from RNA-transfected cells (Yi et al, unpublished data). To monitor replication, the GLuc sequence, fused at its C terminus to the foot-and-mouth disease virus 2A autoprotease, was inserted between p7 and NS2 of pH77S.2 (Supplementary Figure 4). To insert the GLuc-coding sequence between p7 and NS2 in pH77S.2, followed by the foot-and-mouth disease virus 2A protein-coding sequence, Mlu I, EcoR V, and Spe I restriction sites were created between the p7 and NS2 coding sequences by site-directed mutagenesis. DNA coding for GLuc was subcloned into the Mlu I and EcoR V sites of the modified plasmid after PCR amplification using the primers: 5′- ATA ATA TTA CGC GTA *TGG GAG TCA AAG TTC TGT TTG CC*-3′ (sequence corresponding to the N-terminal GLuc is italicized and that corresponding to Mlu I is underlined) and 5′-ATA AAT AGAT ATC *GTC ACC ACC GGC CCC CTT GAT CTT*-3′ (C terminal GLuc is italicized and EcoR V is underlined). A DNA fragment encoding the 17 amino acids of the foot-and-mouth disease virus 2A protein was generated by annealing the following complementary oligonucleotides: 5′- ATA TGA TAT CAA CTT TGA CCT TCT CAA GTT GGC CGG CGA CGT CGA GTC CAA CCC AGG GCC CAC TAG CAT AT-3′ and 5′-ATA TGC TAG TGG GCC CTG GGT TGG ACT CGA CGT CGC CGG CCA ACT TGA GAA GGT CAA AGT TGA TAT CAT AT-3′ (underlined sequences indicate EcoR V and Spe I sites). The annealed oligonucleotides were digested by both restriction enzymes and the product inserted into the corresponding sites of pH77S.2 containing GLuc to generate pH77S.2/GLuc2A. Q41R is a cell-culture adaptive mutation within the NS3 protease domain of pH77S. Because it is not essential for production of infectious virus (Yi et al, unpublished data), pH77S.2 and pH77S.2/GLuc2A constructs underwent this mutation by site-directed mutagenesis of a PCR fragment spanning the Afe I and BsrG I sites to replace Gln_{41} with wild-type Arg. The resulting plasmids (pH77S.2/R41Q and pH77S.2/GLuc2A/R41Q) were redesignated pH77S.3 and pH77S.3/GLuc2A, respectively.[3,4] GLuc has several advantages over other luciferase reporter enzymes in that it is smaller and allows more sensitive detection than either firefly or Renilla luciferase.[3,4] In addition, a signal sequence directs its secretion into cell-culture media, allowing real-time dynamic measurements of GLuc expression without the need for cell lysis. H77S.3/GLuc2A RNA produces infectious virus, although with lower efficiency than H77S.3 RNA (10-fold less).

References

1. Shimbo K, Kubo S, Harada Y, et al. Automated precolumn derivatization system for analyzing physiological amino acids by liquid chromatography/mass spectrometry. Biomed Chromatogr 2009; 24:683–691.
2. Yi M, Villanueva RA, Thomas DL, et al. Production of infectious genotype 1a hepatitis C virus (Hutchinson strain) in cultured human hepatoma cells. Proc Natl Acad Sci U S A 2006;103:2310–2315.
3. Shetty S, Kim S, Shimakami T, et al. Hepatitis C virus genomic RNA dimerization is mediated via a kissing complex intermediate. RNA 2010;16:913–925.
4. Shimakami T, Welsch C, Yamane D, et al. Protease inhibitor-resistant hepatitis C virus mutants with reduced fitness from impaired production of infectious virus. Gastroenterology 2011; 140:667–675.

OPEN ACCESS Freely available online

PLoS one

Development of Mouse Hepatocyte Lines Permissive for Hepatitis C Virus (HCV)

Hussein Hassan Aly[1], Hiroyuki Oshiumi[1], Hiroaki Shime[1], Misako Matsumoto[1], Taka Wakita[2], Kunitada Shimotohno[3], Tsukasa Seya[1]*

1 Department of Microbiology and Immunology, Hokkaido University Graduate School of Medicine, Sapporo, Hokkaido, Japan, **2** Department of Virology II, National Institute of Infectious Diseases, Shinjuku, Tokyo, Japan, **3** Research Institute, Chiba Institute of Technology, Narashino, Chiba, Japan

Abstract

The lack of a suitable small animal model for the analysis of hepatitis C virus (HCV) infection has hampered elucidation of the HCV life cycle and the development of both protective and therapeutic strategies against HCV infection. Human and mouse harbor a comparable system for antiviral type I interferon (IFN) induction and amplification, which regulates viral infection and replication. Using hepatocytes from knockout (ko) mice, we determined the critical step of the IFN-inducing/amplification pathways regulating HCV replication in mouse. The results infer that interferon-beta promoter stimulator (IPS-1) or interferon A receptor (IFNAR) were a crucial barrier to HCV replication in mouse hepatocytes. Although both IFNARko and IPS-1ko hepatocytes showed a reduced induction of type I interferons in response to viral infection, only IPS-1-/- cells circumvented cell death from HCV cytopathic effect and significantly improved J6JFH1 replication, suggesting IPS-1 to be a key player regulating HCV replication in mouse hepatocytes. We then established mouse hepatocyte lines lacking IPS-1 or IFNAR through immortalization with SV40T antigen. Expression of human (h)CD81 on these hepatocyte lines rendered both lines HCVcc-permissive. We also found that the chimeric J6JFH1 construct, having the structure region from J6 isolate enhanced HCV replication in mouse hepatocytes rather than the full length original JFH1 construct, a new finding that suggests the possible role of the HCV structural region in HCV replication. This is the first report on the entry and replication of HCV infectious particles in mouse hepatocytes. These mouse hepatocyte lines will facilitate establishing a mouse HCV infection model with multifarious applications.

Citation: Aly HH, Oshiumi H, Shime H, Matsumoto M, Wakita T, et al. (2011) Development of Mouse Hepatocyte Lines Permissive for Hepatitis C Virus (HCV). PLoS ONE 6(6): e21284. doi:10.1371/journal.pone.0021284

Editor: Jacques Zimmer, Centre de Recherche Public de la Santé (CRP-Santé), Luxembourg

Received May 13, 2011; **Accepted** May 24, 2011; **Published** June 22, 2011

Funding: This work was supported in part by Grants-in-Aid from the Ministry of Education, Science, and Culture (Specified Project for Advanced Research), the Ministry of Health, Labor, and Welfare of Japan, and the Hokkaido University Leader Development System in the Basic Interdisciplinary Research Areas (L station). Supports from Mitsubishi Foundation, Mochida Foundation, NorthTec Foundation Waxman Foundation and Yakult Foundation are gratefully acknowledged. The funders had no role in study design, data collection and analysis, decision to publish, or preparation of the manuscript.

Competing Interests: The authors have declared that no competing interests exist.

* E-mail: seya-tu@pop.med.hokudai.ac.jp

Introduction

Chronic hepatitis C virus (HCV) infection is a major cause of mortality and morbidity throughout the world infecting around 3.1% of the world's population [1]. The development of much needed specific antiviral therapies and an effective vaccine has been hampered by the lack of a suitable small animal model. The determinants restricting HCV tropism to human and chimpanzee hosts are unknown. Replication of HCV strain JFH1 has been demonstrated in mouse cells only upon antibody selection [2], highlighting the very limited replication efficiency. Human CD81 and occludin have been implicated as important entry receptors for retrovirus particles bearing HCV glycoproteins, HCV pseudoparticles (HCVpp), into NIH3T3 murine cells [3]. However, HCV infection, spontaneous replication and particle production by mouse cells have not yet been reported.

In mammalian cells, the host detects and responds to infection by RNA-viruses, including HCV, by primarily recognizing viral RNA through several distinct pathogen recognition receptors (PRRs), including the cell surface and endosomal RNA sensors Toll-like receptors 3 and 7 (TLR3 and TLR7), and the cytoplasmic RNA sensors retinoic acid-inducible gene I (RIG-I) and melanoma differentiation associated gene 5 (MDA5) [4]. The detection of virus infection by these receptors leads to the induction of interferons (IFNs) and their downstream IFN-inducible anti-viral genes through distinct signaling pathways [5]. Type I IFN is an important regulator of viral infections in the innate immune system [6]. Another type of IFN, IFN-lambda, affects the prognosis of HCV infection, and its response to antiviral therapy [7,8].

Mutations impairing the function of the RIG-I gene and the induction of IFN were essential in establishing HCV infectivity in human HuH7.5 cells [9]. Similarly, the HCV-NS3/4a protease is known to cleave IPS-1 adaptor molecule, inducing further downstream blocking of the IFN-inducing signaling pathway [10]. These data clearly demonstrate that the host RIG-I pathway is crucial for suppressing HCV proliferation in human hepatocytes. Using a similar strategy, we investigated whether suppressing the antiviral host innate immune system conferred any advantage on HCV proliferation in mouse hepatocytes. We examined the possibility of HCV replication in mice lacking the expression of key factors that modulate the type I IFN-inducing pathways. Only gene silencing of the IFN receptor (IFNAR) or IPS-1 was sufficient to establish spontaneous HCV replication in

mouse hepatocytes. To establish a cell line permissive for HCV replication, which is required for further *in vitro* studies of the HCV life cycle in mouse hepatocytes, we immortalized IFNAR- and IPS-1-knockout (ko) mice hepatocytes with SV40 T antigen. Upon expression of the human (h)CD81 gene, these newly established cell lines were able to support HCV infection for the first time in mouse hepatocytes. Viral factors required for HCV replication in mouse hepatocytes were also analyzed.

Results

IPS-1-mediated IFN signaling is important for HCV replication in mouse hepatocytes

As a first step in establishing HCV infection in mice, we tested the susceptibility of mouse hepatocytes to persistent expression of HCV proteins after RNA transfection. *In vitro* transcribed chimeric J6JFH1 RNA, in which the HCV structural and non-structural regions were from J6 and JFH1 isolates respectively, was transfected into hepatocytes from wild-type mice. We used a highly sensitive polyclonal antibody derived from HCV-patient serum for the detection of HCV proteins. No HCV proteins were detected five days after transfection (Fig. 1 A), suggesting that wild-type mouse hepatocytes were unable to maintain HCV replication. We then tried to find and block the pathway used by mouse hepatocytes for the detection of viral-RNA and the induction of IFN response. Mouse hepatocytes did not show the expression of either TLR3 or TLR7 as detected by RT-PCR, unlike IPS-1 and RIG-I which was fairly detected (Fig. S1), suggesting that the cytoplasmic RIG-I/IPS-1 pathway is the main pathway utilized by mouse hepatocytes for the detection of RNA viruses. We then checked the susceptibility of hepatocytes from TICAM-1ko, IPS-1ko and IFNARko mice to the prolonged expression of HCV proteins (Fig. 1B–D). Only IPS-1- and IFNARko mouse hepatocytes showed expression of J6JFH1 proteins five days after transfection (Fig. 1), indicating the importance of impaired IPS-1 and/or IFNAR receptors for HCV persistence. Similarly, the detection of the J6JFH1-RNA in transfected hepatocyte lines from various knockout mice showed higher levels in IPS-1 or IFNAR knockout cells compared to TICAM-1knockout cells in which a rapid decline of J6JFH1-RNA levels was noticed similar to the non-replicating control JFH1GND construct (Fig. S2). These data clearly suggest that the RIG-I/IPS-1 but not TLR3/TICAM-1 is the main pathway utilized for the detection of HCV-RNA and the induction of anti-viral immune response in mouse hepatocytes. Its suppression significantly improves HCV replication in mouse hepatocytes.

Establishment and characterization of immortalized mouse hepatocyte cell lines lacking expression of the IFNAR or IPS-1 gene

We further established mouse hepatocyte lines with disrupted IFNAR or IPS-1 genes through immortalization with SV40T antigen, and used these cell lines to study factors required for the HCV life cycle. Hepatocytes were transduced with SV40T-expressing lentivirus vectors. Six weeks after transduction, hepatocytes transduced with SV40T showed continuous proliferation and clonally proliferating hepatocyte lines were selected. SV40T-immortalized IFNARko and IPS-1ko clones were designated IRK (Fig. 2 A) and IPK (Fig. 2 B), respectively. 20 IRK and 19 IPK clones were picked up, of which IRK clones 2 and 4 (IRK2 and IRK4) and IPK clones 10 and 17 (IPK10 and IPK17) were most closely related to primary mouse hepatocytes in term of differentiation (Fig. 2 C) and were used in the following experiments. Expression of SV40T was confirmed by RT-PCR analysis (data not shown). IRK2, IRK4, IPK10 and IPK17, but not the non-hepatocytic NIH3T3 cells, displayed albumin and hepatocyte nuclear factor 4 (HNF4) expression similar to that observed in liver tissue, but did not express the bile duct marker, cytokeratin. IRK and IPK cells did not show expression of IFNAR and IPS-1 respectively (Fig. 2 C).

Replication of the HCV genome in IRK and IPK cells

To assess the permissiveness of the established cell lines to HCV replication, we transduced IRK4 and IPK17 cells with J6JFH1 RNA and monitored the HCV protein and RNA levels by IF (Fig. 3 A) and real time RT-PCR (Fig. 3 B). The number of cells expressing HCV proteins, as detected by IF, increased over time, indicating the continuous proliferation of J6JFH1 in these cells. However, the ratio between infected and non-infected cells did not significantly change over time for 7 days after transfection. Similarly, the amount of total J6JFH1 RNA in 1 μg of total cellular RNA was reasonably constant. By contrast, the level of

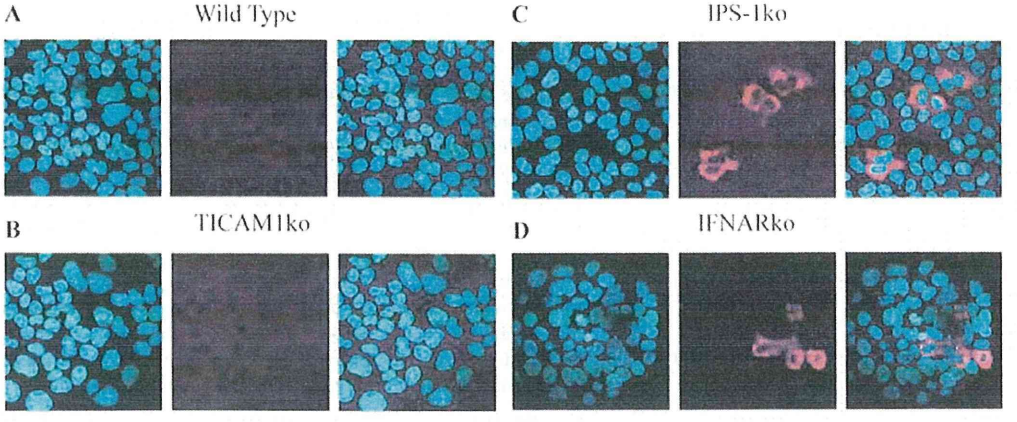

Figure 1. IF detection of of J6JFH1 proteins' expression 5 days after transfection of J6JFH1-RNA through electroporation into wild type (A), TICAM-1ko (B), IPS-1ko (C), and IFNARko (D), freshly isolated primary hepatocytes. A highly sensitive polyclonal antibody extracted from HCV-patient serum (AbS3) was used for the detection. Staining of the uninfected hepatocytes from different Ko mice was also performed and they showed negative for HCV proteins (data not shown).
doi:10.1371/journal.pone.0021284.g001

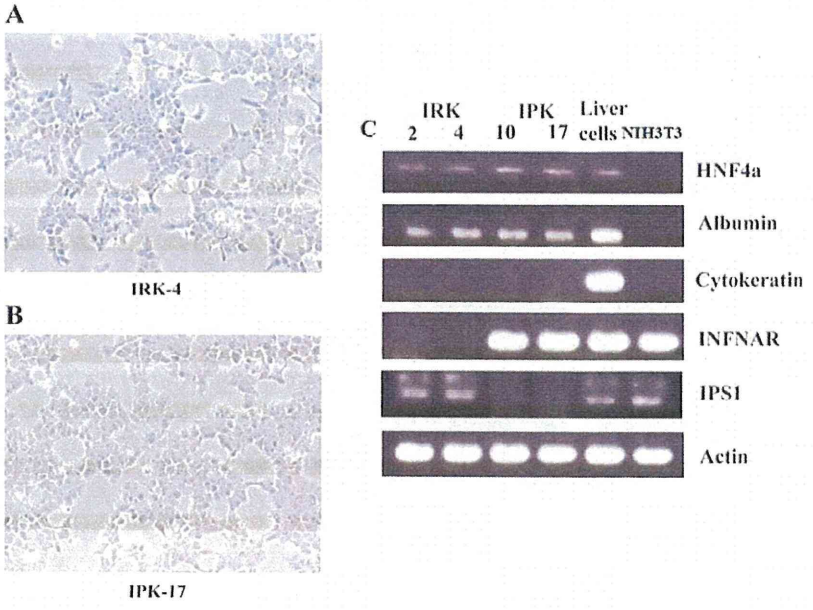

Figure 2. Morphological characteristics of IRK-4 (A) and IPK-17 (B) cells. (C) RT analysis for the expression of albumin, HNF4, cytokeratin, interferon A receptor, and IPS-1 in 2 IFNAR-KO cell lines (IRK2 and 4), 2 IPS-1-KO cell lines (IPK-10 and 17), total liver, and NIH3T3 cells.
doi:10.1371/journal.pone.0021284.g002

JFH1GND RNA carrying a mutation in NS5B hampering HCV replication, rapidly declined, indicating the requirement of continuous HCV replication for the maintenance of HCV positivity in the transfected mouse hepatocytes. Similar data were obtained from IRK2 and IPK10 cells (data not shown).

IPS-1-dependent/Interferon-independent pathway is responsible for HCV's cytopathic effect

In comparison to IPS-1ko hepatocytes, J6JFH1-RNA in IFNARko were lower and decreased further after its transfection, while higher stable levels of J6JFH1-RNA were maintained in IPS-1ko cells (Fig. 3 B and Fig. S2). Similarly, larger numbers of HCV-positive cells were detected in IPS-1ko hepatocytes compared with their IFNARko counterparts (Fig. 3 A), suggesting that the IPS-1 disruption benefits HCV replication in a distinct manner from IFNAR disruption. To measure the interferon induction after RNA virus infection in those cells, we used a highly infectious RNA-Virus (VSV) and measured the induction of interferon after its infection. All the interferons measured showed similar suppression of induction in IFNARko and IPS-1ko hepatocytes (Fig. 4). Surprisingly, cellular cytopathic effect that was monitored after transfection of J6JFH1-RNA was markedly reduced in IPS-1ko but not in IFNARko hepatocytes after transfection (Fig. 5A). This suppression was accompanied by an increase of J6JFH1-RNA levels in IPS-1ko cells, suggesting that minimal cellular damage induced by HCV replication in IPS-1-/- cells led to the improvement of HCV proliferation in mouse hepatocytes (Fig. 5B).Reduction of HCV-induced cellular cytotoxicity (Fig.5C), and improvement of HCV replication (Fig.5D) in wild type, and IFNAR-KO cells were found when we cultured the cells with a pan-caspase inhibitor, zVAD-fmk, 2 days before and after HCV-RNA transfection. We reasoned that the IPS-1 pathway rather than the IFNAR pathway capacitates hepatocytes to induce HCV-derived apoptotic cell death and its disruption resulted in the circumvention of cell death.

Human CD81 is required for HCV infection of mouse hepatocytes

Similar to the primary mouse hepatocytes, immortalized mouse hepatocytes showed the expression of all the mouse counterparts of human HCV entry receptors (Fig. S3). Human CD81 and hOccludin, but not other human HCV receptors such as SR-B1 or claudin1, have previously been reported to be essential for HCVpp entry into NIH3T3 mouse cells [3]. We then expressed hCD81 and/or hOccludin in IRK2 and IRK4 cells using lentivirus vectors. Using a MOI of 10, 95% transfection efficiency was achieved (Fig. S4) with lentivirus vector. We next tested the effect of these proteins on HCV particle (HCVcc) infection. Human CD81 alone was found to be required for J6JFH1 infection into all IRK and IPK cells tested (Fig. S5 and Fig. 6 A, and B). For the first time in mouse hepatocytes, HCV proteins were detected in nearly 1% of the cells used for infection. These data demonstrated the importance of hCD81 in establishing HCVcc infection in mouse hepatocytes.

Viral factors affecting HCV replication in mouse hepatocytes

After successfully establishing J6JFH1 infection in mouse hepatocytes, we attempted to infect these cells with other strains of HCV. Human CD81-expressing IPK17 cells were infected with full-length JFH1FL, however, no infection was detected (data not shown). This might be due to a problem in infection and/or replication. We further examined the replication efficiency of JFH1FL, the subgenomic JFH1 replicon and the J6JFH1 chimera in two different mouse hepatocyte lines and the HuH7.5.1 cell line. The persistent expression of HCV proteins was detected seven days after RNA transfection. Although HCV proteins were detected in HuH7.5.1 cells in all cases (Fig. 7 C), only J6JFH1 proteins were detected in the mouse hepatocyte lines, suggesting for the first time the importance of the J6 structural region for the replication of HCV in mouse hepatocytes (Fig. 7 A, and B).

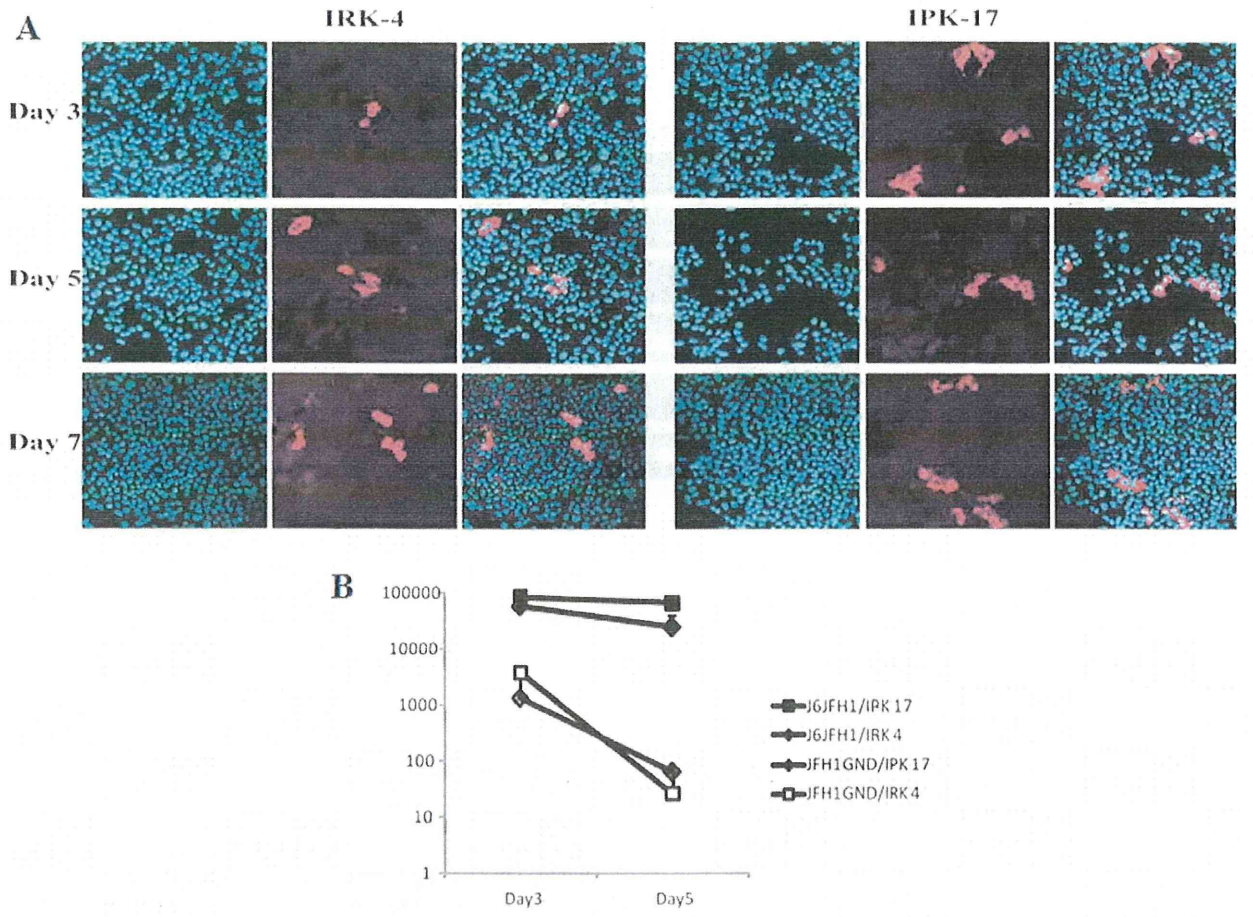

Figure 3. Proliferation of HCV in IRK4 and IPK17 cells over time as detected by immunofluorescence staining of NS5a protein using the CL1 rabbit polyclonal antibody (A) and by quantitative real-time RT-PCR analysis of HCV-RNA levels (B). JFH1GND was used as a negative control to exclude non replicating HCV-RNA. The data plotted represent the average +/− STD of 3 different experiments.
doi:10.1371/journal.pone.0021284.g003

Discussion

Gene silencing of either IPS-1 or IFNAR significantly improves HCV replication and persistence in mouse hepatocytes compared with wild-type or TICAM-1ko mice. This result demonstrated the importance of the IPS-1 pathway rather than the TICAM-1 pathway in the induction of type I IFN by HCV infection, and revealed that the IFNAR amplification pathway confers resistance to HCV in mouse hepatocytes independently of TICAM-1. In accordance with our data, HCV-NS3/4A protease is known to cleave the IPS-1 and/or RIG-I-complement molecules including DDX3 and Riplet in humans to overcome the host innate immune response, showing the importance of RIG-I/IPS-1 pathway suppression in the establishment of HCV infection [10,11,12].

To further study factors affecting the HCV life cycle in mouse hepatocytes, we established IPK and IRK immortalized mouse hepatocyte lines by transduction with SV40T antigen. The established hepatocytes cell lines showed expression of HNF4, a major hepatocyte transcription factor, required for hepatocyte differentiation and liver-specific gene expression [13]. The maintenance of hepatocellular functions was demonstrated by continuous expression of hepatocyte specific differentiation marker, albumin, and the lack of expression of the bile duct marker, cytokeratin. The close resemblance of these cell lines to primary mouse hepatocytes is crucial to ensure the physiological relevance of factors identified in these cell lines that affect the HCV life cycle.

It is worth noting that HCV replication in IPS-1ko was higher than that in IFNARko hepatocytes. Since IPS-1 is present upstream of IFNAR in the IFN-amplification pathway, this higher J6JFH1 replication efficiency in IPS-1ko hepatocytes suggested the presence of an additive factor affecting HCV replication other than the induction of IFNAR-mediated type I IFN. This enhanced replication efficiency was also not accompanied by the induction of other interferon types, but was correlated with the reduction of HCV-induced apoptosis in mouse hepatocytes. This data clearly demonstrates that IPS-1 is playing an important role in the regulation of HCV infection in mouse hepatocytes through two different pathways, the IFN-induction pathways and another new IFN-independent pathway, leading to apoptotic cell death and elimination of HCV-harboring hepatocytes. The cytopathic effect of HCV infection in human cells is still contradictory. Although, some reports showed the induction of apoptosis and cell death by HCV infection in human hepatocytes [14,15,16], others showed suppression of apoptosis by HCV proteins [17,18]. This difference may be due to the different cell lines used in the different studies. Almost all the studies reporting HCV-induced apoptosis used

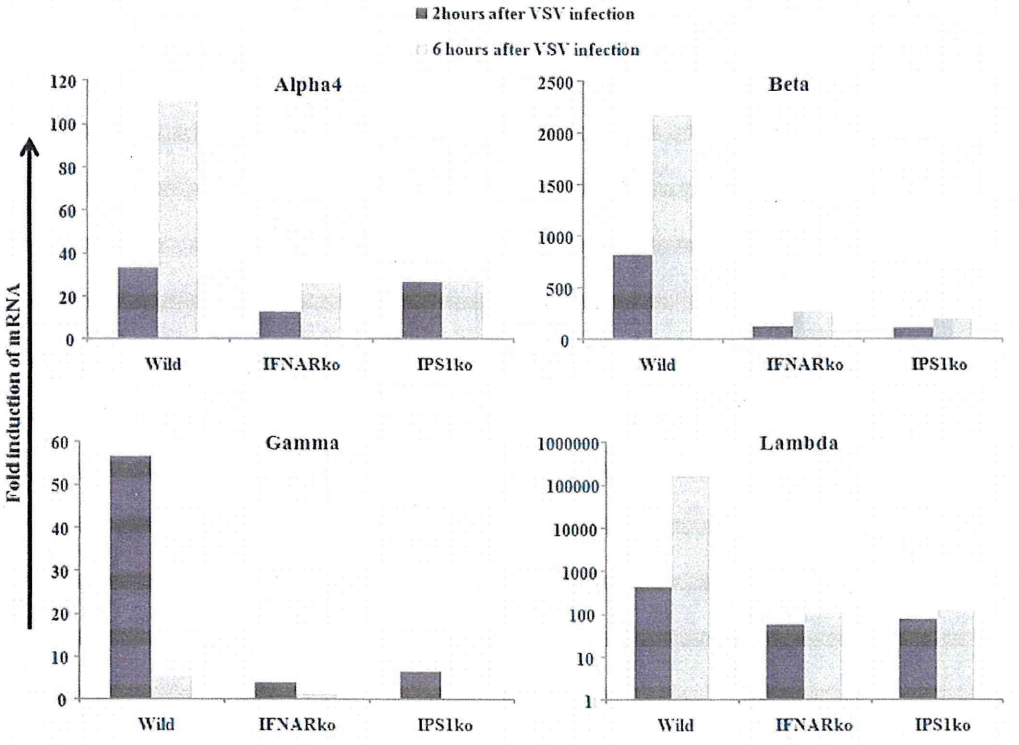

Figure 4. Wild type, IFNARko, and IPS-1ko mice hepatocytes were infected with mock or VSV virus, 2 and 6 hours later, total RNA was extracted from the cells, and interferon alpha, beta, gamma and lambda mRNA induction levels were measured by real-time RT-PCR. Similar results were obtained from 2 different experiments, each was performed in duplicates. The data plotted represent the mean duplicate readings in one of them.
doi:10.1371/journal.pone.0021284.g004

hepatocellular carcinoma cell lines. Since it has been established that the inability to undergo apoptosis is essential for the development of cancer [19,20,21], our use of immortalized, non-cancerous hepatocytes may make it possible to reproduce the physiological response of the cells to HCV infection more closely. The IPS-1 regulation of cell death following the introduction of HCV-RNA may also regulate the effector cell function. It is likely that hepatocyte debris generated secondary to intrinsic production of viral dsRNA in HCV-infected hepatocytes affect the antiviral effector response of the immune system through maturation of dendritic cells [22]. Hence, the effector cell activation may be enhanced by the induction of cell death through the IPS-1 pathway in hepatocytes which may facilitate producing dsRNA-containing debris.

In comparison to the JFH1GND construct with deficient replication that showed a rapid reduction in its RNA levels over time after transfection into mouse hepatocytes, J6JFH1 RNA was detected at four-log higher levels and was maintained at a relatively stable levels in IPS-1ko hepatocytes. Although the number of mouse cells expressing HCV proteins was found to increase over time, as detected by IF, the ratio between HCV-negative and -positive cells did not show any significant change for 7 days after transfection and increased after 10 days (data not shown). This indicates a negative selection of HCV-bearing cells over time which may be due to slower cellular replication, or loss of HCV replication. Another possibility may be that HCV infection is affected by the presence of an inhibitory factor possibly triggered by HCV replication or the lack of a human host factor required for HCV replication. Due to the initial replication of HCV in the transfected IPK and IRK mouse hepatocytes for the first 7 days and the establishment of infection, we favor the presence of a possible inhibitory factor that may be triggered by HCV replication. Another factor that also limits HCV spread in mouse hepatocytes is the failure of HCV to produce infectious particles in these cells (data no shown).

Using this newly established immortalized mouse hepatocyte line, we found that although J6JFH1, JFH1FL and the subgenomic JFH1 replicon all share a similar non-structural region derived from isolate JFH1 that is required for HCV replication, and although all of these constructs can replicate efficiently in HuH7.5.1 cells, strikingly, only J6JFH1 carrying the J6 structural region replicated in mouse hepatocytes. This indicates the importance of the J6 structural region and/or the chimeric construct between J6 and JFH1 for HCV replication in mouse hepatocytes. Structural regions are known to be important for HCV entry and/or particle formation [23], but this is the first time that their importance in replication in HCV-bearing cells has been demonstrated. This finding clearly shows the importance of non-hepatoma cell lines with less genetic abnormalities and mutations for the discovery of new aspects of the life cycle of HCV.

Although, the co-expression of human CD81 and Occludin genes was found to be important for HCVpp entry into murine NIH3T3 cells [3], the expression of hCD81 alone was sufficient for J6JFH1 entry into mouse hepatocytes. This may be explained by the different cell lines used in the different studies. In contrast to NIH3T3 cells, we used immortalized hepatocytes that showed close physiological resemblance to primary mouse hepatocytes and showed the expression of all the mouse counterparts of HCV entry

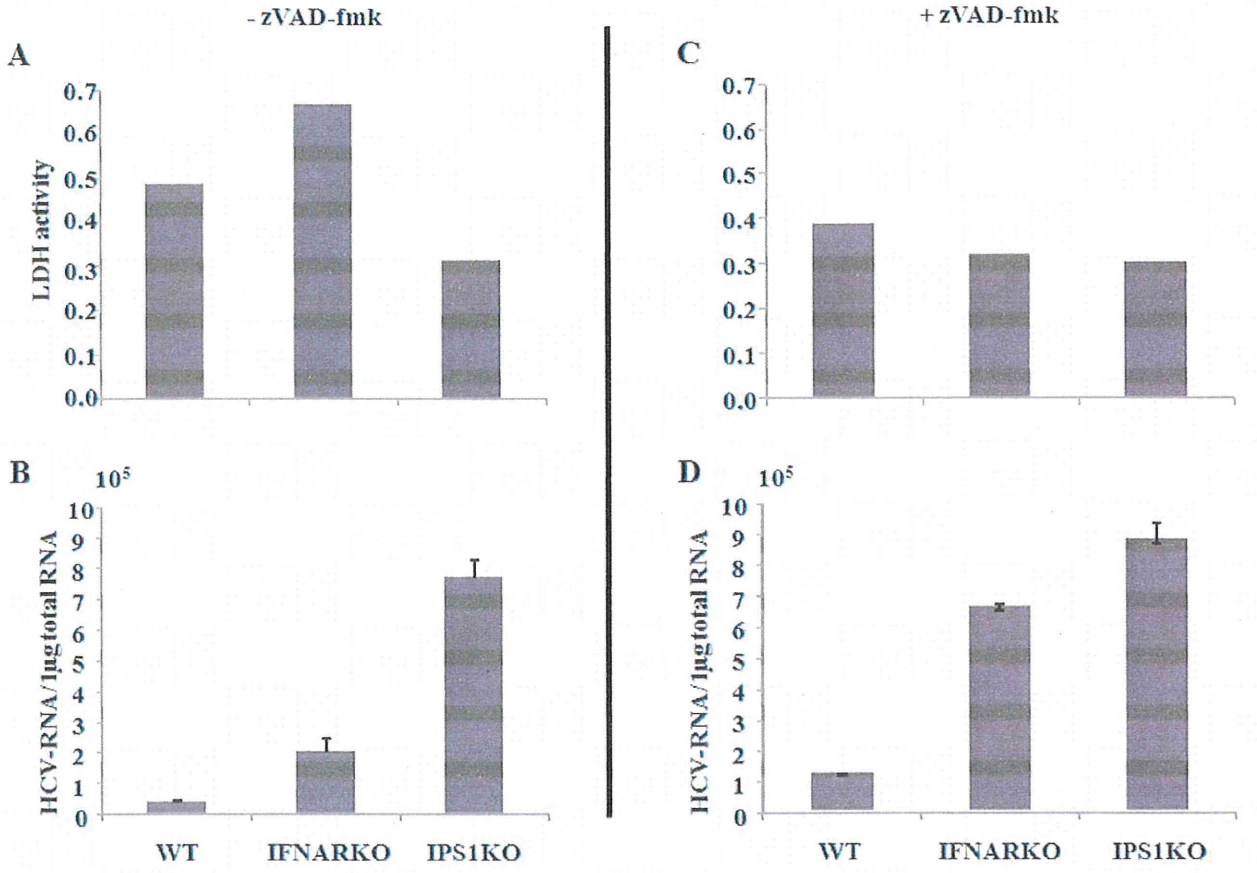

Figure 5. Measurement of J6JFH1 mediated cytopathic effect in wild type, IFNARko, and IPS-1ko mouse hepatocytes. Cultrure medium were left untreated (A;B) or treated with 20 μM of zVAD-fmK (C;D) 2 days before and after J6JFH1-RNA transfection. One day after transfection of J6JFH1-RNA, culture medium was discarded and cells were washed with PBS. A new medium was added and cells were cultured for another 24 hours. The LDH activity in the culture medium was measured in 2 different experiments in duplicates and showed similar results, the average levels of a duplicate from a single experiment was plotted (A, C). HCV-RNA titers in the cells were also measured using real-time RT-PCR (B, D), the data shown represent the mean +/− STD of 3 different experiments.
doi:10.1371/journal.pone.0021284.g005

receptors. A study from a different group showed that adaptive mutations in HCV envelope proteins allowing its interaction with murine CD81 is enough for efficient HCVpp entry without the expression of any human entry receptors in murine cells [24]. This report, together with ours, suggest that CD81 is the main human host restriction factor for HCV entry, and that overcoming this problem either by HCV adaptation to murine CD81, or the expression of human CD81 in murine hepatocytes is essential for HCV entry. Although our lentivirus transfection efficiency with CD81 was around 95% in IPK and IRK clones, only 1% of the cells were prone to infection with HCVcc. Also, HCVpp showed lower entry levels in those cells compared to HuH7.5.1 cells (Fig. S6). This suggests that hCD81 expression is the minimum and most crucial requirement for HCV entry into mouse hepatocytes. The discovery and expression of other co-receptors facilitating HCV entry in human cells is still required for efficient and robust HCV infection.

In summary, the suppression of IPS-1 is important for the establishment of HCV infection and replication in mouse hepatocytes through the suppression of both interferon induction and interferon independent J6JFH1-induced cytopathic effect. We have established hepatocytes lines from IPS-1 and IFNARko mice that support HCV replication and infection. These cell lines will be very useful in identifying other species restriction factors and viral determinants required for further establishment of a robust and efficient HCV life cycle in mouse hepatocytes. Using those cells, we showed for the first time the importance of HCV structural region for viral replication. IRF3ko mouse embryo fibroblasts (MEFs) were previously shown to support HCV replication more efficiently than wild MEFs [25]. Since the knockout of IPS-1 mainly suppresses signaling in response to virus RNA detection, and maintains an intact IFN response to other stimulants, it may result in minimum interference to adaptive immune responses as compared to IRF3 or IFNARko. Therefore, further development of hCD81-transgenic IPS-1ko mice may serve as a good model for the study of immunological responses against HCV infection. This mouse model can be used as a backbone for any further future models supporting robust HCV infectivity for the study of HCV pathogenesis, propagation and vaccine development.

Material and Methods

Cell culture

HuH7.5.1 cells were cultured in high-glucose Dulbecco's modified Eagle's medium (DMEM; Gibco/Invitrogen, Tokyo, Japan) supplemented with 2 mM L-glutamine, 100 U of penicillin/ml, 100 μg of

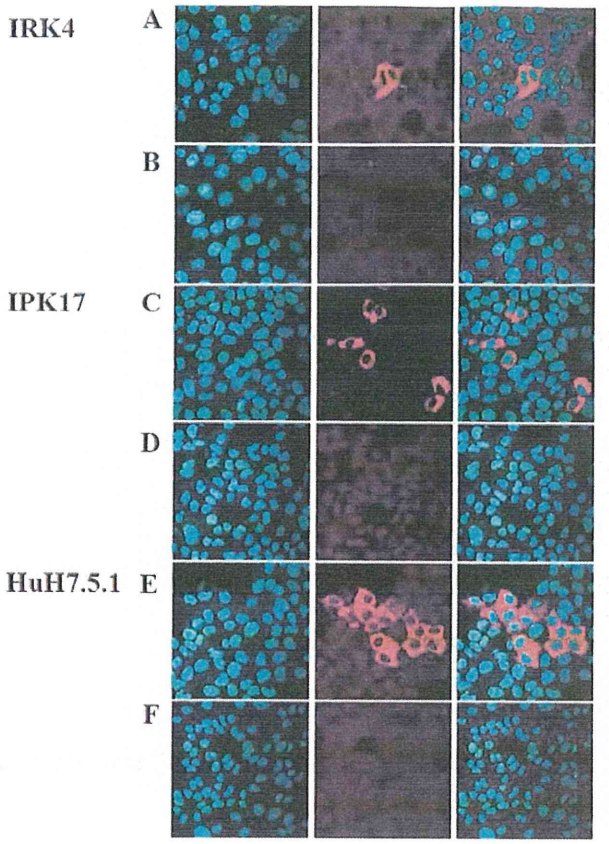

Figure 6. J6JFH1 infection into IRK-4 and IPK17 cells. HCV-NS5A protein detection in mouse IRK4 (A,B) and IPK17 (C,D) and human 7.5.1 cells (E,F). The cells were transduced with lentivirus expressing human CD81 gene at 10 MOI. 48 hours later the cells were infected with 100 times concentrated supernatant medium, collected during 1 week after transfection of HuH7.5.1 cells with J6JFH1-RNA (A, C, and E) or JFH1GND-RNA (B, D, and F).
doi:10.1371/journal.pone.0021284.g006

streptomycin/ml and 10% fetal bovine serum. Mouse primary hepatocytes were isolated from the liver using collagenase perfusion through the inferior vena cava (IVC), while clamping the animal's intrathoracic extension. Hepatocyte isolation and perfusion control were performed as previously described [26]. Primary and immortalized hepatocytes were cultured in a similar medium supplemented with: HEPES (Gibco/Invitrogen), 20 mmol/L; L-proline, 30 μg/mL; insulin (Sigma, St. Louis, MO, USA), 0.5 μg/mL; dexamethasone (Wako, Osaka, Japan), 1×10^{-7} mol/L; $NaHCO_3$, 44 mmol/L; nicotinamide (Wako), 10 mmol/L; EGF (Wako), 10 ng/mL; L-ascorbic acid 2-phosphate (Wako), 0.2 mmol/L; and MEM-non essential amino acids (Gibco/Invitrogen), 1%.

Gene-disrupted mice

All mice were backcrossed with C57BL/6 mice more than seven times before use. Toll-like receptor adaptor molecule 1 (TICAM-1) ko [27] and IPS-1ko mice [28] were generated in our laboratory (detailed information regarding the IPS-1 mice will be presented elsewhere). All mice were maintained under specific-pathogen-free conditions in the animal facility of the Hokkaido University Graduate School of Medicine (Japan).

RNA extraction, reverse transcriptase polymerase chain reaction (RT-PCR) and real-time RT-PCR

RNA was extracted from cultured cells using Trizol reagent (Invitrogen, San Diego, CA, USA) according to the manufacturer's protocol. Using 1 μg of total RNA as a template, we performed RT-PCR and real-time RT-PCR as previously described [29,30].

In vitro RNA transcription, transfection and preparation of J6JFH1 and Jfh1 viruses

In vitro RNA transcription, transfection into HuH7.5.1 or mouse hepatocytes, and preparation of J6JFH1 and JFH1 viruses, were all performed as previously reported [31]. RNA transfection into human and mouse hepatocytes was performed by electroporation using a Gene Pulser II (Bio-Rad, Berkeley, California) at 260 V and 950 Cap.

HCV infection

J6JFH1 and JFH1 concentrated medium were adjusted to contain a similar RNA copy number by real-time RT-PCR. 2×10^4 cells/well were cultured in 8-well glass chamber slides. After 24 hours, the medium was removed and replaced by concentrated medium containing JFH1 or J6JFH1 viruses. After three hours, the concentrated medium was removed, cells were washed with PBS and incubated in fresh medium for 48 hours, before the detection of infection.

Lentivirus construction, titration and infection

The gene encoding T antigen from simian virus was cloned from plasmid CSII-EF-SVT [32]. The genes encoding human CD81 and occludin were cloned from HuH-7.5.1 cells using the Zero Blunt TOPO PCR Cloning Kit (Invitrogen) according to the manufacturer's protocol. These genes were then inserted into the GFP reporter gene-containing lentiviral expression (pLBIG) vector using the *Eco*RI and *Xho*I restriction sites for SV40T and hCD81, and the *Xba*I and *Xho*I restriction sites for hOccludin. Lentivirus expression vectors were then constructed as previously described [27]. GFP expression was used for the titration of lentivirus vectors, and a multiplicity of infection (MOI) of 10 was used for the infection of mouse cells. Forty-eight hours after the transfection of hCD81 and/or hOccludin, cells were trypsinized and counted. Then, 2×10^4 cells/well were cultured in 8-well glass chamber slides for HCV infection and 5×10^4 cells/well were cultured in 12-well plates, along with 1 ml of medium containing HCVpp, for HCV entry experiments.

HCVpp construction and the detection of luciferase expression

HCVpp containing the E1 and E2 proteins from HCV isolate J6 and expressing the luciferase reporter gene were a kind gift from Dr. Thomas Pietschmann at the TWINCORE Center for Experimental and Clinical Infection Research, Germany. The production of HCVpp and the measurement of luciferase levels were performed as previously described [33].

Indirect immunofluorescence (IF)

IF expression of HCV proteins was detected in the infected cells using antibodies in the serum of chronic HCV patients or rabbit IgG anti-NS5A antibody (Cl-1) (both kind gifts from K. Shimotohno, Chiba Institute of Technology, Japan). Goat anti-human IgG Alexa 594 and goat anti-rabbit Alexa 594 (Invitrogen) were used as secondary antibodies, respectively. Fluorescence

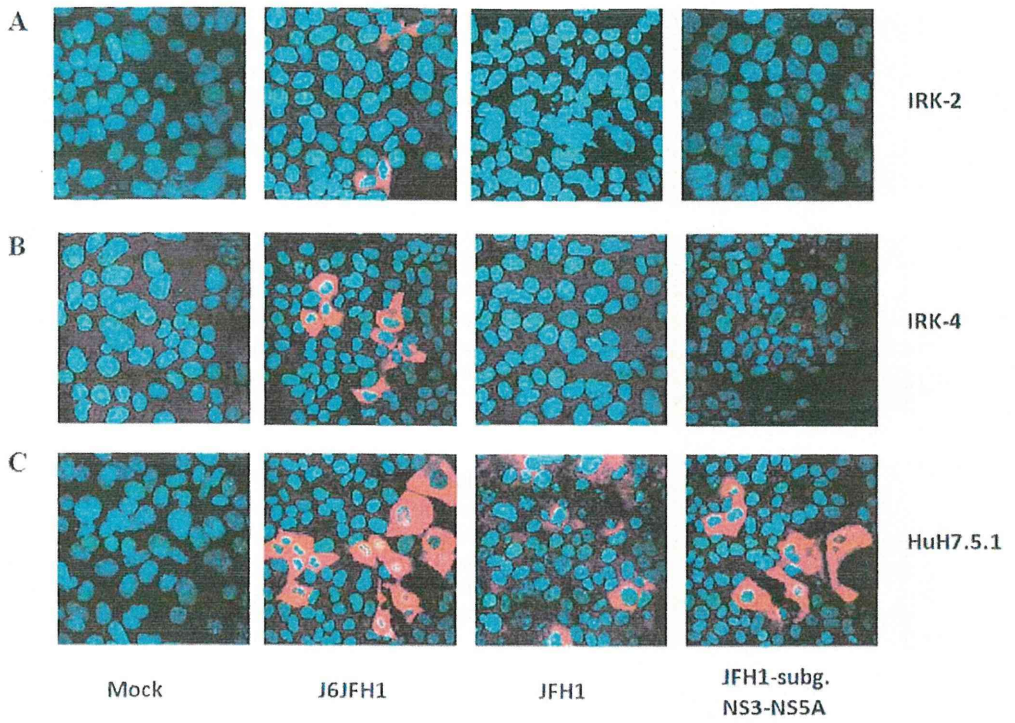

Figure 7. Detection of HCV-NS5A protein in IRK-2 (A), IRK-4 (B) and HuH-7.5 cells (C) by IF 5 days after transfection with J6JFH1, FL-JFH1 or subgenomic JFH1-RNA.
doi:10.1371/journal.pone.0021284.g007

detection was performed on a ZEISS LSM 510 Meta confocal microscope (Zeiss, Jena, Germany).

Detection of cell death

Culture medium was collected from HCV infected and control cells and used for measuring lactate dehydrogenase (LDH) levels using an LDH cytotoxicity detection kit (Takara Biomedicals, Tokyo, Japan). Light absorbance was then measured according to the manufacturer's protocol.

Ethic Statement

This study was carried out in strict accordance with the recommendations in the Guide for the Care and Use of Laboratory Animals of the National Institutes of Health. The protocol was approved by the Committee on the Ethics of Animal Experiments in the Animal Safety Center, Hokkaido University, Japan. All mice were used according to the guidelines of the institutional animal care and use committee of Hokkaido University, who approved this study as ID number: 08-0243, " Analysis of immune modulation by toll-like receptors".

Supporting Information

Figure S1 RT detection of TLR3, TLR7, RIG-I, and IPS-1 expression in mouse hepatocytes. GAPDH expression was used as internal control, and RNA from CD11c+ spleenocytes (dendritic cells) was used as positive control.
(TIF)

Figure S2 Proliferation of HCV in IPS-1, TICAM-1(TRIF) and IFNAR-knockout mouse hepatocytes over time as detected by quantitative real-time RT-PCR analysis of HCV-RNA levels. JFH1GND transfection into IPS-1 knockout cells was used as a negative control to exclude non replicating HCV RNA. The data plotted represent the average +/− STD of 3 different experiments.
(TIF)

Figure S3 RT detection of CD81, Occludin, Claudin 1, SRB1, and LDL receptor expression in primary, IRK4 and IPK17 mouse hepatocytes. GAPDH expression was used as internal control.
(TIF)

Figure S4 Estimation of the transfection efficiency of lentivirus vector expressing green fluorescent protein (GFP) as a reporter, together with hCD81 or hOccludin. 48 hours after transfection with the lentivirus vector, cells were trypsinized and GFP positive cells were detected by BD FACSCalibur (BD Biosciences).
(TIF)

Figure S5 HCV infection of IRK2 cells transfected with lentivirus expressing hCD81 and/or hOccludin. IRK2 cells were transfected with lentivirus expressing empty vector (A), hCD81 (B), hOccludin (C) or hCD81 and hOccludin (D) at a MOI of 10. After 48 hours, the cells were infected with concentrated J6JFH1 transfected 7.5.1 culture medium. After a further three hours, cells were washed with PBS and incubated in fresh medium. After another 48 hours, HCV infection was examined through the detection of HCV-NS5a protein expression by immunofluorescence staining.
(TIF)

Figure S6 HCVpp entry into mouse cells. A similar number of IPK17 and HuH7.5.1 were cultured in triplicate. IPK17 cells were only transfected with lentivirus expressing hCD81, while HuH7.5.1 cells were transfected with empty vector at a MOI of